Lawrence Berkeley National Laboratory
Recent Work

Title
COMPOSITE SEMICONDUCTOR BOLOMETERS FOR THE DETECTION OF FAR-INFRARED RADIATION

Permalink
https://escholarship.org/uc/item/1hw0m3kg

Author
Nishioka, Norman S.

Publication Date
1976-12-01

eScholarship.org Powered by the California Digital Library
University of California

UU UU ... UU ... // UU ... UU UU

LBL-5774
c.1

COMPOSITE SEMICONDUCTOR BOLOMETERS FOR THE DETECTION OF FAR-INFRARED RADIATION

Norman S. Nishioka
(M. S. thesis)

December 1976

Prepared for the U. S. Energy Research and Development Administration under Contract W-7405-ENG-48

For Reference

Not to be taken from this room

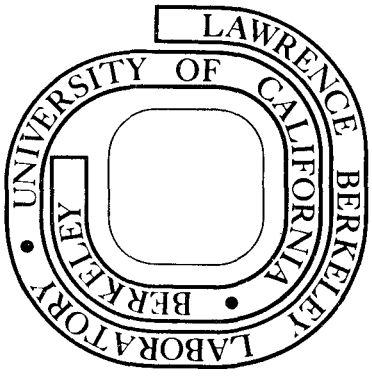

LBL-5774
c.1

DISCLAIMER

This document was prepared as an account of work sponsored by the United States Government. While this document is believed to contain correct information, neither the United States Government nor any agency thereof, nor the Regents of the University of California, nor any of their employees, makes any warranty, express or implied, or assumes any legal responsibility for the accuracy, completeness, or usefulness of any information, apparatus, product, or process disclosed, or represents that its use would not infringe privately owned rights. Reference herein to any specific commercial product, process, or service by its trade name, trademark, manufacturer, or otherwise, does not necessarily constitute or imply its endorsement, recommendation, or favoring by the United States Government or any agency thereof, or the Regents of the University of California. The views and opinions of authors expressed herein do not necessarily state or reflect those of the United States Government or any agency thereof or the Regents of the University of California.

0 0 0 0 4 7 0 4 5 5 4

COMPOSITE SEMICONDUCTOR BOLOMETERS FOR THE DETECTION OF FAR-INFRARED RADIATION

Norman S. Nishioka

Department of Physics, University of California, and
Molecular and Materials Research Division
Lawrence Berkeley Laboratory, Berkeley, California 94720

ABSTRACT

A composite semiconductor bolometer for the detection of far-infrared radiation has been developed in which doped germanium serves as the temperature sensor and a bismuth coated sapphire substrate serves as the radiation absorber. Metal wires serve as the thermal and electrical conductance to the environment. These detectors operate at pumped liquid ^{4}He temperatures ($\sim$ 1.3 K). In many applications these detectors approach the theoretical limits of sensitivity.

Optimization calculations have been performed which predict both the ultimate performance possible from these detectors as well as the optimum operating conditions in various experimental situations.

0000 0044770040565556

ACKNOWLEDGEMENTS

I feel extremely fortunate to have come under the direction of Professor P. L. Richards. I am truly indebted to him for his patience, understanding, and kindness as well as his many clever suggestions.

I would also like to thank Dr. David Woody for his countless suggestions and criticisms. Dr. Eugene Haller provided many helpful hints for the preparation of the germanium and Robert Bailey provided the software expertise to make the noise measurements possible.

This work was performed under the auspices of the U. S. Energy Research and Development Administration.

00 00 00 00 44 77 00 40 55 67

Table of Contents

0 0 0 0 4 7 0 4 5 5 8

I. INTRODUCTION

Bolometers have long been widely used as detectors of far-infrared radiation. The first detection of infrared radiation was made by Herschel[1] in 1800. His bolometer was simply a conventional mercury thermometer which registered an increased temperature when illuminated by infrared radiation. However, the term "bolometer" was not used until 1880 when Langley[2] used the term to refer to a fine wire which acted as a thermal detector by changing its resistance in response to a changing temperature. At the time of its introduction, Langley's resistance bolometer provided a significant increase in the sensitivity of infrared detectors.

Developments in recent years have enabled bolometers to be built whose performance in many applications approaches the theoretical limits of sensitivity. These developments include the introduction of the semiconductor bolometer by Low[3] in 1961, the SNS tunnel junction bolometer of Clarke et al.[4,5], and the superconducting transition edge bolometer developed by several workers[6,7]. At present, the semiconductor bolometer is the most widely used detector in the far-infrared. Among the chief reasons for its popularity are commercial availability, the straightfoward electronics required for its operation, and its ability to operate in high magnetic fields.

A bolometer can be viewed as performing three different functions. It acts as a thermometer, a radiation absorber and often as a mode limiter. In order to optimize the bolometer performance for a given experimental

situation, it is necessary to optimize all three of these functions. In most semiconductor bolometers used at present all three of these functions are performed by a single element so that independent optimization of each function is difficult. For example, the resistance of the semiconductors used in composite semiconductor bolometers at low temperatures follows $R = R_o e^{\Delta/T}$ where R_o and Δ are constants. As we will see high responsivity demands that Δ be large. However, at frequencies ν such that $h\nu < k\Delta$ (h is the Planck constant, k the Boltzmann constant), the absorption of the germanium is small. Thus, we see that the demands of high responsivity and high absorption are in conflict.

In an attempt to surmount these difficulties, we have built bolometers that relegate these functions to different elements, hence the term composite bolometer. It should be noted that this trend toward separation of the various functions of a bolometer is not a novel idea. Similar attempts have been made in the past with varying degrees of success[8]. The composite semiconductor bolometers described here employ gallium doped germanium as the thermometer and bismuth coated sapphire substrates as the absorbing element.

These bolometers have a wide variety of applications. They have been sucessfully used for Fourier transform spectroscopy as well as in a balloon-borne cosmic background experiment. Anticipated applications include far-infrared astronomy from mountain top observatories as well as from balloon-borne telescopes.

0 0 0 0 4 7 0 4 5 5 8

II. OPTIMIZATION

A. Introduction

There are many different approaches to the problem of optimizing the performance of a bolometer for a specific observing situation. Each approach has its advantages as well as its shortcomings. In this section the approaches that we have found particularly convenient will be discussed. In addition, some applications of these formulas to other types of bolometers will be mentioned.

It should be pointed out that the design of the optimal bolometer depends crucially upon the particular observing situation. The bolometer that is optimum for use in one application may be a poor choice for use in a different situation. Since bolometers exhibit this application specificity, it is important to characterize each application carefully. We have found that the dc background radiation power is adequate to parameterize most observing situations. However, in certain applications the chopping frequency may be of importance. This is particularly true in the presence of large amounts of 1/f noise. Note also that the chopping frequency is not always determined by detector requirements alone since other factors such as the stability of the source must be considered.

For our purposes here, a bolometer will be defined to be any radiation detector whose output is an electrical signal and which operates in the following way. The radiation is detected by absorbing it, degrading it to heat and monitoring the associated temperature rise via some parameter (such as resistance) which alters the electrical output. Therefore, a photoconductor is not a bolometer since the changing output signal is not due to a temperature change.

B. Numerical Methods

As the first step in the analysis, we examine the sources of noise in a bolometer. An appropriate figure of merit is the noise equivalent power (NEP). The NEP is the incident power required to yield a signal-to-noise ratio of unity in a 1 Hz post detection bandwidth. The NEP can be written as the rms sum of several terms[9]

$$(NEP)^2 = \frac{4kTR}{S^2} + \frac{4kT^2G}{\varepsilon^2} + \frac{8\sigma k A T^5}{\varepsilon} + \frac{4\varepsilon\varepsilon' (kT_{rad})^5 A\Omega}{c^2 h^3}\int_{x_1}^{x_2} \frac{x^4 e^x}{(e^x - 1)^2}\, dx$$

$$+ F(R,T,G,I,\varepsilon,\ldots). \qquad (1)$$

The first term is the Johnson noise voltage developed across the bolometer (whose resistance is R and which operates at the temperature T) divided by the square of the (optical) responsivity S (volts/watt). Here k is the Boltzmann constant. The second term is the square of the phonon fluctuation noise power. The bolometer is connected to a heat sink (at temperature T_s) through a thermal conductance G. The third term represents the random fluctuactions in the emission from the bolometer itself. The bolometer has an area A and an emissivity ε. σ is the Stefan-Boltzmann constant. The fourth term is the square of the noise associated with the radiant power incident on the bolometer. The background is at a temperature T_b, has an emissivity ε' and is viewed through the (effective) solid angle Ω. We have assumed that a square filtering system has been used so that the integral is carried out from the low frequency cutoff ν_1 to the high frequency cutoff ν_2. We have used the variable $x = h\nu c/kT_{rad}$ where c is the speed of light and h is Planck's constant. The last term represents all additional noise in the detector system such as 1/f noise, amplifier noise, etc.

0 0 0 0 4 7 0 4 5 5 0

In most systems $T << T_{rad}$, so that we can neglect the third term in (1). It should be noted that, given any fixed frequency interval, the fluctuations in the incident power form a fundamental limit to the NEP. We will adhere to the terminology of Low and Hoffman[9] by referring to a detector whose NEP is dominated by the fluctuations in the incident radiation as ideal. In addition, the term dark electrical NEP will refer to an NEP calculated using only the first two terms in (1) and using the electrical responsivity ($\varepsilon = 1$ in Eq. (18)) instead of the optical responsivity. The term real dark electrical NEP will refer to an NEP calculated by adding the function F to the dark electrical NEP. Once again, the electrical responsivity enters into F instead of the optical responsivity. The ideal (or background limited) NEP is of course computed from the fourth term in (1) (see Appendix A). Finally, the term optical NEP will refer to the NEP computed from the first four terms of (1). Thus,

$$(NEP)^2_{\text{dark electrical}} = \frac{4kTR}{S^2_{\text{electrical}}} + 4kT^2G, \tag{2}$$

$$(NEP)^2_{\text{real dark electrical}} = (NEP)^2_{\text{dark electrical}} + F(\varepsilon=1,R,T,G,I,\ldots), \tag{3}$$

$$(NEP)^2_{\text{background fluctuation}} = \frac{4\varepsilon\varepsilon'(kT_{rad})^5 A\Omega}{c^2h^3}\int_{x_1}^{x_2} \frac{x^4e^x}{(e^x-1)^2}\,dx, \tag{4}$$

$$(NEP)^2_{\text{optical}} = \frac{4kTR}{S^2} + \frac{4kT^2G}{\varepsilon^2} + (NEP)^2_{\text{background fluctuation}}, \tag{5}$$

$$(NEP)^2_{\text{real optical}} = (NEP)^2_{\text{optical}} + F(R,T,G,I,\varepsilon,\ldots). \tag{6}$$

In much of the analysis to follow the dark electrical NEP (2) will be the object of the optimization process. The optimized $(NEP)_{DE}$ that results

will then be compared to $(NEP)_{BF}$ (4) to see how close the system comes to being ideal. Of course, it is more realistic to use the real dark electrical NEP (3) in these considerations. Unfortunately, the function F is often not well known and can vary considerably from bolometer to bolometer. However, in certain cases an empirical formula for F can be deduced and the optimization can be carried out using (3).

In order to carry the analysis any further, we need an expression for the responsivity of a bolometer. We begin by conserving the energy flowing to and from the bolometer.

$$C \frac{dT}{dt} + G(T - T_s) = \varepsilon(P_o + P_s) + W, \tag{7}$$

where the bolometer is assumed to be isothermal with the temperature T, have a heat capacity C and be connected to a temperature sink at the temperature T_s through a thermal conductance G. The bolometer absorbs a fraction ε of the incident radiation $P_o + P_s$. P_o is the dc radiation power incident upon the bolometer and P_s represents the signal to be detected. W is the electrical joule heating occuring in the bolometer. In the steady state with $P_s = 0$, (7) becomes

$$T_o = T_s + \frac{\varepsilon P_o + W(T_o)}{G(T_o)}, \tag{8}$$

where T_o is the static or dc operating temperature. We have explicitly written W and G as evaluated at $T = T_o$ since they are, in general, functions of temperature.

We now define the temperature rise due to the signal power P_s as

$$\delta = T - T_o. \tag{9}$$

With this definition, (7) can be written

$$C \frac{d\delta}{dT} + G\left[\delta + \frac{\varepsilon P_o + W(T_o)}{G(T_o)}\right] = \varepsilon(P_o + P_s) + W. \tag{10}$$

0 0 0 0 4 7 0 4 5 6 9

W can be expanded to first order about T_o to yield

$$W \approx W(T_o) + \frac{dW}{dT}\,\delta. \tag{11}$$

In addition, if G is assumed to be temperature independent, then (10) and (11) can be combined to yield

$$C\frac{d\delta}{dt} + (G - \frac{dW}{dT})\delta = \varepsilon P_s\,. \tag{12}$$

The assumption that G is temperature independent is reasonable for small values of δ (which is equivalent to requiring that the signal be small). The Wiedemann-Franz law[10] states that the ratio of the thermal conductivity to the electrical conductivity is proportional to the temperature. At low temperatures the electrical conduction is impurity limited and is thus independent of temperature. Therefore, most metals exhibit a thermal conductance that is linear in temperature. However, certain evaporated metal films have exhibited[5] a thermal conductance proportional to T^4 to T^5. Also hidden by the assumption of a temperature independent thermal conductance is the fact that the temperature varies along the element providing the thermal conductance. Therefore, if G is temperature dependent it will vary from $G(T_s)$ to $G(T)$ along the thermal path. This difficulty can however be easily handled due to a theorem[11] which states that the heat flow H between two bodies at different temperatures T_1 and T_2 is given by

$$H = \int_{T_1}^{T_2} G(T)\,dT. \tag{13}$$

Thus the correct result can be obtained by using the average conductivity between the two temperatures T_1 and T_2.

For the case of a sinusoidally varying signal power $P_s = P_s e^{i\omega t}$,

(12) can be solved for δ by the substitution $\delta = \delta_o e^{i\omega t}$. The result is

$$\delta_o = \frac{\varepsilon P_s}{G_{eff} + i\omega C} , \tag{14}$$

where

$$G_{eff} = G - \frac{dW}{dT} . \tag{15}$$

G_{eff} is called the effective thermal conductance and provides a convenient method for taking the thermal feedback of the system into account. Note that if $G_{eff} < 0$ then the solution of (12) has an exponentially increasing solution when $P_s = 0$. Therefore, if the bolometer is to be thermally stable, G_{eff} must be positive.

Defining the effective time constant $\tau = C/G_{eff}$ yields

$$\left|\frac{\delta_o}{P_s}\right| = \frac{\varepsilon}{G_{eff}(1 + \omega^2\tau^2)^{\frac{1}{2}}} . \tag{16}$$

The responsivity is

$$S = \frac{dV}{dP_s} ,$$

$$= \frac{dV}{dx}\ \frac{dx}{dT}\ \frac{dT}{dP_s} , \tag{17}$$

where V is the output voltage of the detector. Here x is the temperature dependent property of the bolometer, such as the bolometer resistance in a semiconductor or superconducting transition edge bolometer. By combining (16) and (17) we obtain an expression for the optical responsivity

$$|S| = \frac{dV}{dx}\ \gamma\ \frac{\varepsilon}{G_{eff}(1 + \omega^2\tau^2)^{\frac{1}{2}}} , \tag{18}$$

where we have written $\gamma = dx/dT$. Here γ is the temperature derivative of

0 0 0 0 4 7 0 4 5 6 2

the bolometer's temperature dependent parameter.

For a semiconductor bolometer, the resistance is a rapidly varying function of temperature and can be written

$$R(T) = R_o e^{\Delta/T} . \tag{19}$$

Typical values of R_o and Δ are $R_o \sim 1\ k\Omega$, $\Delta \sim 10$ K. In usual operation, a semiconductor is biased with a constant current so that (18) becomes

$$|S_{elec}| = \frac{I\gamma}{G_{eff}(1 + \omega^2\tau^2)^{\frac{1}{2}}} , \tag{20}$$

where I is the bias current.

Armed with (2) and (20), the optimization of a semiconductor bolometer can be performed. We rewrite (2) with the help of (8), (15), and (20)

$$(NEP)_{DE} = \frac{4k\left(T_s + \frac{\varepsilon P_o + I^2R}{G}\right)R(G_{eff} + \omega^2C^2)}{I^2\gamma^2} + 4k\left(T_s + \frac{\varepsilon P_o + I^2R}{G}\right)^2 G, \tag{21}$$

where $G_{eff} = G - I^2\gamma$.

There are several things to note. First, since $\gamma = -R\Delta/T^2$, G_{eff} is always a positive number. Thus a constant current biased semiconductor bolometer is unconditionally thermally stable. Second, the heat capacity C should be made as small as possible to minimize the NEP. Therefore, the heat capacity is not normally considered to be a free parameter in the optimization. One exception to this is when the size of the bolometer is of importance in the analysis. In addition, the sink temperature should be made as low as possible and γ should be made as large as possible.

Several variations of the optimization procedure result from the selection of which parameters are considered free and which are considered determined by the experiment. There are of course no universal rules so that each individual experiment will dictate its own set of free and fixed parameters. For example, in our laboratory we have access to doped germanium that has $\Delta \sim 10$ K which we operate at pumped liquid ^{4}He temperatures (~ 1.3 K). The free parameters for this situation are taken to be I, G, and R. R is considered to be free since $R = R_o e^{\Delta/T}$ and R_o can be controlled by the geometry of the germanium thermometer. However, values of R in excess of ~ 5 MΩ are inconvenient in actual use. These problems stem from the requirement for constant current bias that the load resistance R_L must be >> R. Also, high values of R cause preamplifier noise to become dominant since the current noise of an amplifier is proportional to the source impedance. All other parameters can be considered fixed. The optimization for this case has been performed on a digital computer. The resulting optimized NEP as a function of the dc background radiation power P_o is shown in Figure 1.

Up until now we have discussed the optimization in terms of designing the optimum bolometer for a given situation. However, we can equally well consider the problem of how to best use a given (non-optimal) bolometer in a given situation. This predicament often arises when the attempts to build the optimum bolometer fall short of their goals. This problem can also be of interest if one chooses to use the same bolometer for several different applications. The former problem often occurs in experiments which are detector noise limited and the latter often occurs in bolometers designed for general lab use.

0 0 0 0 0 4 7 0 4 5 3 2

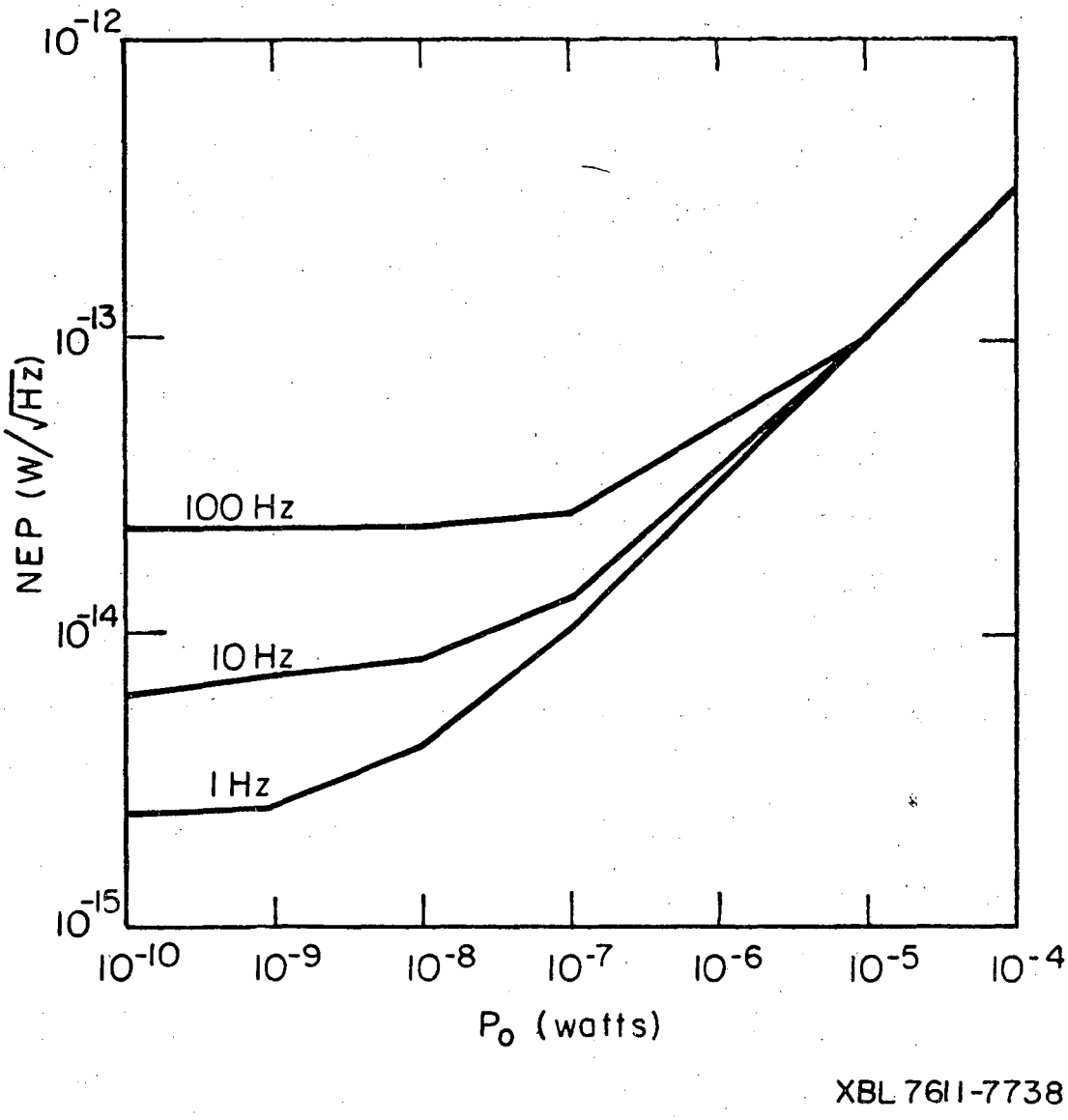

Fig. 1. Optimized NEP as a function of the dc background radiation power for a composite semiconductor bolometer.

An example which illustrates the problems involved is afforded by the balloon-borne cosmic background experiment of Woody et al.[12]. In this experiment, the dc background power is extremely small, $P_o \sim 10^{-12}$ watts and the background limited NEP is also small $(NEP)_{BF} \sim 10^{-16} W/\sqrt{Hz}$. The best detectors available all fall short of this requirement by about a factor of 100. Since the experiment is detector noise limited, it is of importance to obtain the smallest dark optical NEP possible. The noise of the system was measured as a function of several parameters (T,R,I). In addition, the temperature dependances of R, C, and G were measured. All this information was then fed into a computer and a minimization of the NEP was performed to find the optimum bias current. Details of this procedure will be discussed in the section on measurements.

Setting up the optimization problem on a digital computer is usually straightforward. All that is required is to minimize the NEP as a function of the free variables. The minimization of a function of several variables is a common problem and quite elaborate algorithms have been developed. In general, it is desirable to use an algorithm that does not require the partial derivatives of the NEP with respect to the free parameters to be externally calculated since this simplifies the programming considerably. One such algorithm that we have found satisfactory is the conjugate gradient method with internally approximated gradients[13]. Another useful algorithm is the simplex method given by Nelder and Mead[14].

Difficulties may occasionally arise when the optimized NEP, computed by either of the above algorithms gives unphysical results. For example, the "optimized" NEP may occur at a negative value of the thermal conduc-

0 0 0 0 0 7 0 0 6 6 4 3

tance. Constraints also cause difficulties. For example, we require that $G_{eff} > 0$ for stability. In certain bolometers the thermal feedback is positive so that $G_{eff} < 0$ is a possibility. Such possibilities must be excluded from the optimization process. Also, it may be desirable to minimize the NEP subject to the condition that the dynamic range is above some required value. This is particularly true of superconducting transition edge bolometers. When constraints of these sorts must be taken into consideration, a Monte Carlo minimization is usually more effective.

An example of an alternate type of bolometer which lends itself to the above analysis is the critical current or superconducting tunnel junction bolometer[4,5]. In this bolometer, the Josephson critical current I_c in a superconducting-normal-superconducting (SNS) junction is a sensitive function of the temperature. The critical current of the SNS junction is of the form

$$I_c(T) = I_o\, e^{-\sqrt{\frac{T}{T_o}}} . \tag{22}$$

Typically $T_o \sim 0.1$ K and $I_o \sim 1$ amp.

When the SNS bolometer is biased by a constant current I, (18) becomes

$$S = \frac{-R\varepsilon\gamma}{G_{eff}(1 + \omega^2\tau^2)^{\frac{1}{2}}} , \tag{23}$$

where we have assumed that $V = (I - I_c)R$. In this case, $\gamma = dI_c/dT$ and $G_{eff} = G - IR\gamma$. Note that $\gamma < 0$, so that the bolometer is thermally stable in all cases. In practice the resistance is quite small ($R \sim 3 \times 10^{-6}\Omega$) so that $G_{eff} \approx G$ to good approximation. The optimization procedure exactly parallels the procedure used in the optimization of semiconductor bolometers.

C. Large Signal Analysis

The expressions we have been using for the responsivity assume that the signal power P_s is small and sinusoidally varying in time. Also, the thermal conductance and heat capacity were assumed to be temperature independent. When the signal is large, δ, the associated temperature rise may be a large fraction of T. In this case, the temperature dependence of the thermal conductance and heat capacity may be important. In situations such as this (20) will give erroneous values for the responsivity. In order to analyze the bolometer output under these conditions, it is easiest to numerically solve the first order ordinary differential equation resulting from the conservation of energy [Eq.(7)]. The problem is usually reasonably well-conditioned so that a rather straightforward low order numerical technique (such as a low order Euler method) yields satisfactory results. Once the temperature as a function of time is determined, the output voltage as a function of time can be computed from the resistance as a function of temperature R(T). This technique is also of value in predicting the response of a bolometer in situations where non-linear effects are important. An example is the use of large non-sinusoidal signals such as large radiation pulses.

Although this technique is rigorously correct since no approximations are necessary, it is somewhat wasteful of computer time. Therefore, its use is usually limited to cases in which the small signal approximation is not appropriate.

0 00 0 00 04 47 70 0 46 56 65 4

D. Analytical Solutions to the Optimization Problem

Analytical solutions to the optimization problem are in general quite algebraically involved due to the complexities of the formulas and the fact that several variables must be optimized simultaneously. It is usually easier to find the solution numerically since the problem can be solved on a digital computer in a straightforward manner. In addition, many features that are very difficult to include analytically such as the presence of 1/f and preamplifier noise and the temperature dependence of G, C, and R, are very easily incorporated in a numerical treatment. In spite of these shortcomings analytical solutions can be of value in certain situations. For instance, examination of the optimization problem in a few limiting cases can indicate the type of parameter dependence (or independence) expected in these regimes. Even though the approximations involved may cause the constants of proportionality to be in error, the way in which the optimized NEP scales with various parameters may be correct.

A limiting case of interest is where the background radiation power is larger than the joule heating occuring in the bolometer. For a constant current biased semiconductor bolometer (or superconducting transition edge bolometer) this means that $P_o >> I^2R$. In this case, (8) gives

$$T = T_s + \frac{P_o}{G} , \tag{24}$$

where we have assumed that $\varepsilon = 1$ for simplicity. Here I^2 and G are conveniently renormalized as follows:

$$I^2 = -\frac{AP_o}{\gamma T_s} , \quad G = \frac{BP_o}{T_s} , \tag{25}$$

where A and B are dimensionless constants. Note that both G and $\gamma = \frac{dR}{dT}$ are assumed to be independent of temperature[15].

Taking $\omega = 0$ for simplicity, (21) becomes

$$N \equiv \frac{(NEP)^2_{\text{dark electrical}}}{4K} = -\frac{P_o R}{A\gamma}(1+\frac{1}{B})(A+B)^2 + T_s P_o (1+\frac{1}{B})^2 B. \quad (26)$$

The optimized NEP occurs at values of A and B such that

$$\frac{\partial N}{\partial A} = \frac{\partial N}{\partial B} = 0 \ . \quad (27)$$

The differentiations are simple and the result is

$$A^2 = B^2 = \frac{1}{1 - \frac{4R}{\gamma T_s}} \ . \quad (28)$$

For a semiconductor bolometer $\gamma/R = -\Delta/T^2 \sim -\Delta/T_s^2 = -1/T_s T^*$ where $T^* \equiv T_s/\Delta$. In most cases[16], $T^* << 1$ so that (28) becomes

$$A = B \sim 1 - 2T^* \ . \quad (29)$$

Substitution into (26) yields the following result correct to first order in T^*,

$$(NEP)^2_{\text{dark electrical optimum}} \sim 16\, k\, P_o T_s (1 + 2\, T^*). \quad (30)$$

The important feature here is that the optimized NEP is proportional to the square root of the dc background radiation power. If the optical radiation is from a source in the Rayleigh-Jeans limit, then the background limited NEP can be written (see Appendix A)

$$(NEP)_{BF} = 2\, kT_{rad} P_o \ . \quad (31)$$

The summation of (30) and (31) yield the optical NEP of a system with $P_o >> I^2R$,

$$(NEP)^2_{\text{optical optimum}} \sim 2kP_o[8T_s(1+2T^*) + T_{rad}] \ . \quad (32)$$

0 00 0 00 04 47 70 00 46 56 65

Thus if $T_s << T_{rad}$ and $T^* << 1$, the bolometer will be "ideal". That is, its NEP will be dominated by fluctuations in the incident radiation.

The opposite case in which $I^2R >> P_o$ is also of interest. In this case the dc operating temperature becomes

$$T_o = T_s + \frac{I^2R}{G} \quad . \tag{33}$$

Substitution of (33) directly into (21) as we did in the previous cases gives rather unwieldly equations during the minimization process. These problems can be circumvented if we further assume that

$$\frac{I^2R}{G} << T_s \ , \tag{34}$$

which is equivalent to requiring $T_s \approx T$. This restriction limits the range of G so that G will not be considered a free variable. With these assumptions (21) becomes

$$N \equiv \frac{(NEP)^2}{4k} = \frac{RT_s(G - x\gamma)^2}{x\gamma^2} + T_s^2G \ , \tag{35}$$

where $x \equiv I^2$.

Minimizing N as a function of x yields

$$\frac{\partial N}{\partial x} = \frac{RT_s}{\gamma^2}\left[-\frac{2x(G - x\gamma)\gamma - (G - x\gamma)}{x^2}\right] = 0 \quad \Rightarrow x = -G/\gamma \ . \tag{36}$$

Substituting (36) into (35) yields

$$(NEP)^2 = 4kGT_s^2(1 + 4T^*) \ . \tag{37}$$

Thus the optimized dark NEP is limited by the phonon fluctuation noise if $T^* << 1$. Note that in this limit the NEP is independent of P_o.

Using (31) and (37) the optical NEP in the Rayleigh-Jeans limit becomes

$$(NEP)^2_{opt} = 4kGT_s^2(1 + 4T^*) + 2P_okT_{rad} \ . \tag{38}$$

Consequently, if $P_o T_{rad} >> 2GT_s^2(1+4T^*)$ then the bolometer will be in the ideal limit. Note however that (38) was derived assuming that $I^2R << T_s$ and $I^2R >> P_o$. Thus (38) only applies when $GT_s >> I^2R >> P_o$. We can also conclude that, $GT_s >> I^2R >> P_o >> GT_s(\frac{2T_s}{T_{rad}})(1 + 4T^*)$ and $T^* << 1$ are sufficient to guarantee an ideal bolometer.

We can summarize the above results as follows,

$$(NEP)^2_{\text{dark electrical optimum}} \propto \begin{cases} P_o T_s & P_o >> P_{\text{electrical}} \\ T_s^2 & P_o << P_{\text{electrical}} \end{cases} \tag{39}$$

These general results are in qualitative agreement with numerical calculations (cf. Fig. 1). Note also that as the sink temperature is lowered (to say ^{3}He temperatures), the improvement will be more dramatic for the case in which the dc background radiation is very small ($P_o << P_{\text{electrical}}$).

0 0 0 0 0 4 3 9 8 8 9 6

III. CONSTRUCTION AND MEASUREMENT

A. Introduction

The major obstacle that we face in constructing semiconductor bolometers is in securing appropriate semiconductor material. Our laboratory is not equipped to prepare the doped semiconductor material required. Although a gigantic industry has evolved around semiconductors and the technology is extremely advanced, manufacturers are reluctant to develop suitable semiconductor material for this application because of the relatively small market. In addition, preparing the necessary material is not as simple as merely specifying a certain doping level in germanium. The relationship between the doping concentration and the required low temperature parameters such as γ, R, and the low frequency noise are not well understood. Furthermore, most materials suppliers are not equipped to perform low temperature measurements.

We have access to several different boules of germanium which are doped with different materials and in different concentrations. These boules are usually doped with a doping concentration gradient. This permits many different types of low temperature behavior to be achieved in a single boule.

In this section, the construction details of the bolometers that we have built will be given. In addition, the techniques used to evaluate the bolometer's performance will be described.

B. Construction

We have access to several different boules of germanium but the germanium we use most frequently is gallium doped and has a low temperature resistance that very closely follows $R = R_o e^{\Delta/T}$ with $\Delta \sim 10°K$. R_o can be adjusted by varying the dimensions of the germanium and the placement of the electrical leads, but is $\sim$ 1 kΩ for uniform current flow in a cubic sample 1 mm on a side.

The composite semiconductor bolometers that we use consist of a piece of germanium to which two metal wires are soldered. These wires provide both the electrical and the dominant thermal contact to the bolometer. This germanium thermometer is then attached to a sapphire substrate. Nylon threads laced around the substrate provide mechanical rigidity. A bismuth layer is evaporated on one side of the sapphire substrate to increase the absorption of radiation[5]. This structure is attached to a brass ring which serves as the bolometer holder (see Fig. 2).

The initial step in constructing these bolometers is the cutting of an appropriate piece of germanium from the boule. This is done by using a 0.010" stainless steel wire saw with 1900 grit in mineral oil as the abrasive. The sliced germanium is then lapped on all sides with 1900 grit in water to give each face an even finish. The germanium slice is typically $\sim$ 1 mm × 1 mm × 0.3 mm. This size was selected as a compromise between minimizing the heat capacity and providing ease of handling. As we saw in a previous section, optimization requires that the heat capacity be made as small as possible. Thus, ideally the germanium should be made as small as practical. Note however that below a certain germanium volume the heat capacity of the entire bolometer will be

0 0 0 0 0 1 4 7 0 0 4 5 6 7

dominated by other components such as the sapphire substrate, metal leads, etc. In our case, the heat capacity is dominated by the metal leads and sapphire substrate when the germanium volume is $\lesssim 3 \times 10^{-4}$ cm^3. The germanium is next etched with an acid (20:1 HNO_3:HF) for approximately 10 minutes and is quenched in methanol. The germanium is now ready to solder. The wire leads are attached to the germanium with indium solder using Ruby Fluid^{Tm} (mostly $ZnCl_2$) as a flux. This is done using a 10 watt soldering iron equipped with a copper nib. The bolometer is then boiled in distilled water for 5 minutes to remove any residual flux. Next, the sapphire substrate is notched and mounted to a brass ring using 12 μm diameter monofilament nylon threads. Then a layer ($\sim$ 900 Å) of bismuth is evaporated onto the sapphire to act as the absorber.

The germanium with the leads attached is then cemented to the sapphire using Stycast^{Tm} 2850 FT epoxy as the adhesive. Finally, the free ends of the bolometer leads are soldered to the copper pads on the brass ring.

This completes the construction procedure and the bolometer is ready for testing.

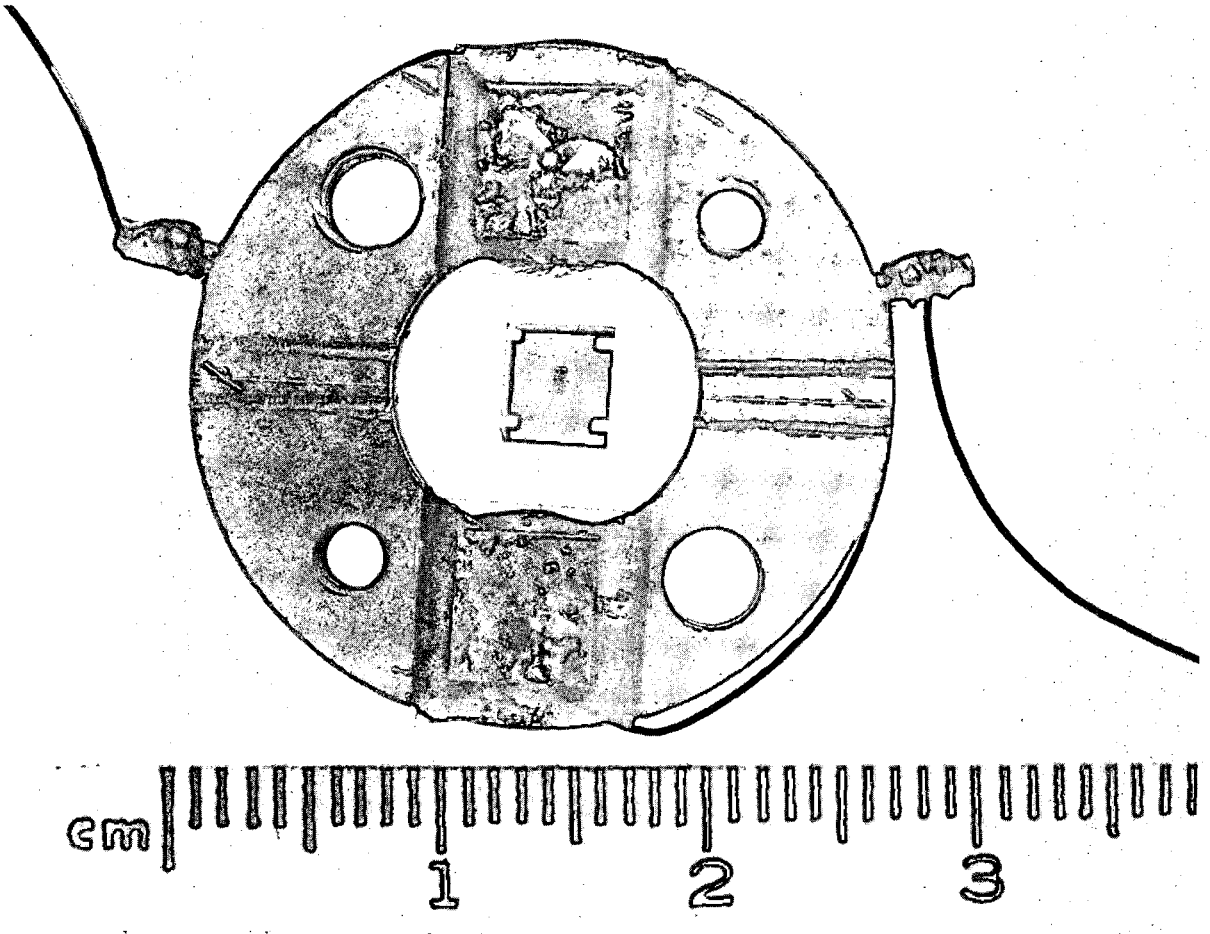

XBB 7512-9203

Fig. 2a. Composite bolometer mounted on a brass ring.

0 0 0 0 0 1 4 7 0 4 5 6 8

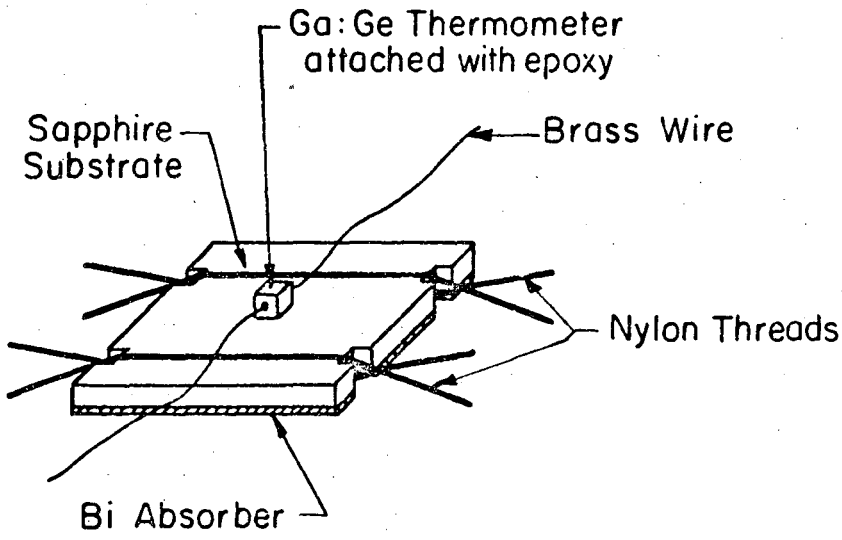

COMPOSITE Ge BOLOMETER

XBL 7611-7706

Figure 2b

C. Testing Procedure

The first measurement made on a bolometer is usually the determination of the curve of resistance as a function of temperature. This is done with the bolometer bathed in liquid helium or helium vapor rather than a vacuum to ensure that the bolometer temperature is equal to the bath temperature. The resistance is monitored by a Keithley 610B electrometer and the bath temperature is monitored by measuring the helium vapor pressure above the bath. The data are then fed into a computer and a best fit (in the least squares sense) to the expression $R = R_o e^{\Delta/T}$ is made with R_o and Δ as the free parameters. As we will see later in this section, it is not necessary to know the resistance-temperature characteristic in order to determine the bolometer performance. However, knowing this characteristic is valuable as a diagnostic tool.

The next step to be made is the characterization of the dark (i.e. no optical radiation) performance of the bolometer. The current-voltage characteristic (I-V curve) is measured using a Keithley 160B digital multimeter to monitor the current and a Keithley 610B electrometer to monitor the voltage. The bolometer is biased by a mercury battery whose output voltage is adjusted by a wirewound potentiometer. This voltage is applied across the series combination of a helium cooled, wirewound load resistor (5 MΩ) and the bolometer. The time constant is measured by applying a small ac voltage in series with the bias voltage. The resulting bolometer output signal then exhibits the familiar $e^{-t/\tau}$ roll-off in amplitude with time associated with a time constant τ. This is the (effective) time constant of the bolometer $\tau = C/G_{eff}$. These two measurements (I-V curve and τ) allow the electrical responsivity to be

0 0 0 0 0 0 0 0 0 0 0

calculated. This is true since the only input power to the bolometer is the electrical heating IV. Thus the I-V curve yields the resistance as a function of the applied power. We represent this function as $\mathcal{R}(P)$. We first solve for a value of the resistance R_1 such that

$$R_1 = \mathcal{R}(I^2 R_1 + P_o + P_s) \ .$$

Next we solve for a value of the resistance such that

$$R_o = \mathcal{R}(I^2 R_o + P_o) \ .$$

The dc responsivity is then

$$S(0) = \frac{I(R_1 - R_o)}{P_s} \tag{40}$$

Note that the responsivity given by (40) is a function of the signal power P_s. In the derivation of (20) we considered the limit where $P_s \to 0$. (40) is not restricted to this limitation. To find the responsivity at the frequency ω, the dc responsivity must be multiplied by $(1 + \omega^2\tau^2)^{-\frac{1}{2}}$.

Alternatively, the electrical responsivity can be measured with the bridge circuit proposed by Jones[17]. The details of this circuit are given in Appendix C.

The measurement of the I-V characteristic, the time constant, and the resistance-temperature characteristic permit the computation of the heat capacity and the thermal conductance. Knowledge of the resistance as a function of the temperature and the resistance as a function of the applied power allows the power as a function of temperature to be deduced. The thermal conductance is the derivative of this function

$$G = \frac{dP}{dT} \ . \tag{41}$$

The heat capacity can be computed from the time constant

$$C = \tau_{eff} \, G_{eff} \ . \tag{42}$$

In order to complete the dark characterization of the bolometer its noise must be measured. We do this with the aid of a PDP-11 computer interfaced to the detector system. The computer samples the voltage output of the detector preamplifier at periodic intervals and computes the Fourier transform to give the noise spectrum. The measured dark NEP is just the ratio of the voltage noise to the responsivity.

D. Results

In this section we will examine a specific bolometer and see how the theory of the previous sections can be applied in an actual situation.

Recall that the design of a bolometer is critically dependent upon the intended application. The bolometer we will examine in this section was designed for use in conjunction with the balloon-borne liquid helium cooled far-infrared spectrophotometer of Woody[12] et al. This experiment, which is designed for observing the cosmic background radiation presents a unique set of detector requirements. The dc radiation power is extremely small ($\sim 10^{-12}$ watts) so that the ideal NEP is quite small ($NEP_{ideal} \sim 10^{-16}$ w/$\sqrt{Hz}$). The chopping frequency of the system is 17 Hz. At float altitude the atmosphere pressure is $\sim$ 2 mm Hg which corresponds to a liquid helium bath temperature of 1.4 K. Unfortunately the exact pressure drop between the environment and the helium cryostat interior is difficult to predict. This means that the helium bath temperature cannot be predicted to better than about $\pm$ 0.15 K. Therefore, the NEP and responsivity as a function of T_s must be known. In addition, since the bias

0 0 0 0 0 4 7 0 0 3 5 7 0

level is preset on the ground prior to flight, it is important to choose the bias current so that the NEP is as close to optimum as possible over this range of T_s. This obviously involves a compromise in performance. We trade optimum performance at a single bath temperature for a more modest but uniform performance over a range of T_s. Furthermore, since this experiment is an absolute measurement, calibration plays an important role. Calibration is accomplished by means of an ambient temperature blackbody source. The consequence of this is that dc background radiation increases considerably during calibration which causes the responsivity to change. Predicting the corresponding change in bolometer responsivity and correcting for it is clearly important.

The bolometer used in this experiment was constructed using two 0.001" diameter brass wires $\sim$ 1 cm long. This results in a thermal conductance of 1×10^{-7} W/K at 1.4 K. The measured time constant is 25 msec. The bolometer resistance closely follows $R = R_o e^{\Delta/T}$ with $R_o \sim 7.2$ kΩ and $\Delta \sim 7.4$ K.

The preamplifier is conveniently modeled by a source resistance, a voltage noise source and a current noise source as indicated in Fig. 3. The voltage noise of the output of the preamplifier is

$$N^2 = 4kTR_s + V_n^2 + I_n^2 R_s^2 .$$

The first term is the Johnson noise due to the source resistance R_s. The noise added by the preamplifier is thus

$$N^2_{preamp} = V_n^2 + I_n^2 R_s^2 .$$

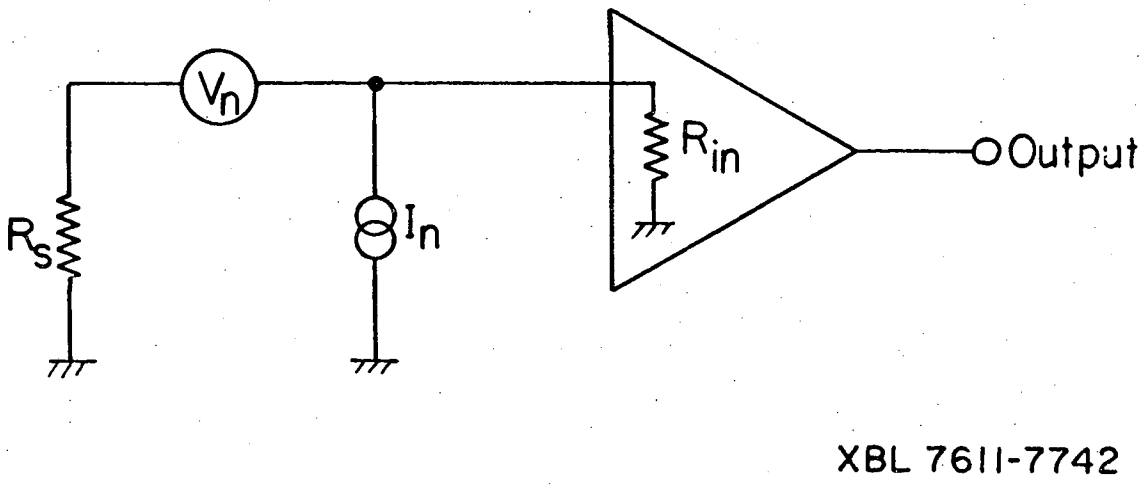

Fig. 3. Noise model for an FET preamplifier.

0 0 0 0 0 4 7 0 4 5 7 2 1

V_n is deduced by measuring the preamplifier noise with $R_s = 0$ (i.e. with the input shorted), and is typically proportional to $1/\sqrt{f}$. Repeating the measurement with a cold resistor connected to the input yields I_n^2.

The particular preamplifier used in this experiment has a bandpass filter with a peak frequency of 17 Hz. Figure 4 shows a typical noise spectrum of the preamplifier. Measurements indicate that $V_n = 5.0$ nV/$\sqrt{\text{Hz}}$ (at 17 Hz), and $I_n = 6 \times 10^{-15}$ amps/$\sqrt{\text{Hz}}$. Thus the amplifier contributes a noise term to the $(\text{NEP})^2$ of $[4.2 \times 10^{-16}/f + 1.9 \times 10^{-29} R^2]/S^2$ where R is the bolometer resistance.

The noise of the bolometer was measured under various temperature and bias conditions and it was empirically found that the excess noise of the bolometer (i.e. noise in excess of Johnson and thermal fluctuaction noise) roughly fit the formula $(\text{NEP})_{\text{excess}} \sim 1.5 \times 10^{-12} R^2 I^2/fS^2$ (W^2/Hz), where I is the bias current and S is the responsivity. Figure 5 shows typical noise spectra for this bolometer.

Using all of the above information, it is possible to use a digital computer to predict the bolometer performance as a function of bias current and sink temperature. With this knowledge, a bias current can be selected and the responsivity under all observing conditions can be determined. Typical performance for this bolometer at 17 Hz and $T_s \sim 1.2$ K is $(\text{NEP})_{\text{real dark electrical}} \sim 3 \times 10^{-14}$ W/$\sqrt{\text{Hz}}$ and responsivity $S \sim 1.7 \times 10^6$ V/W. The Johnson noise term contributes 1.0×10^{-14} W/$\sqrt{\text{Hz}}$, the phonon fluctuation term is 3×10^{-15} W/$\sqrt{\text{Hz}}$, the preamplifier contributes 1.6×10^{-14} W/$\sqrt{\text{Hz}}$ and the excess noise in the bolometer is 2.2×10^{-14} W/$\sqrt{\text{Hz}}$.

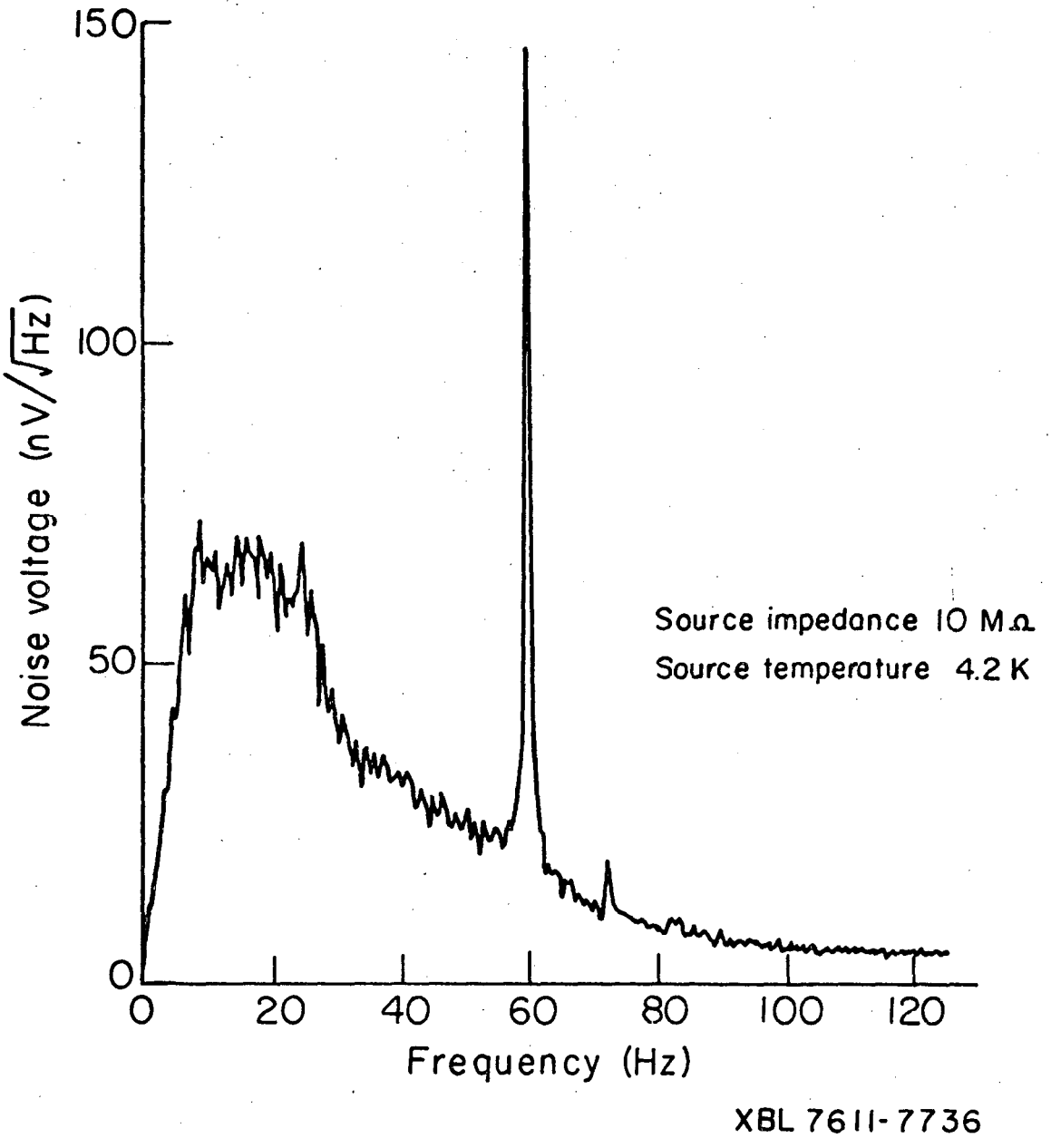

Fig. 4. Typical noise spectrum of the FET preamplifier. Note the effect of the 17 Hz bandpass filter.

0 0 0 0 0 4 7 0 4 5 7 3 2

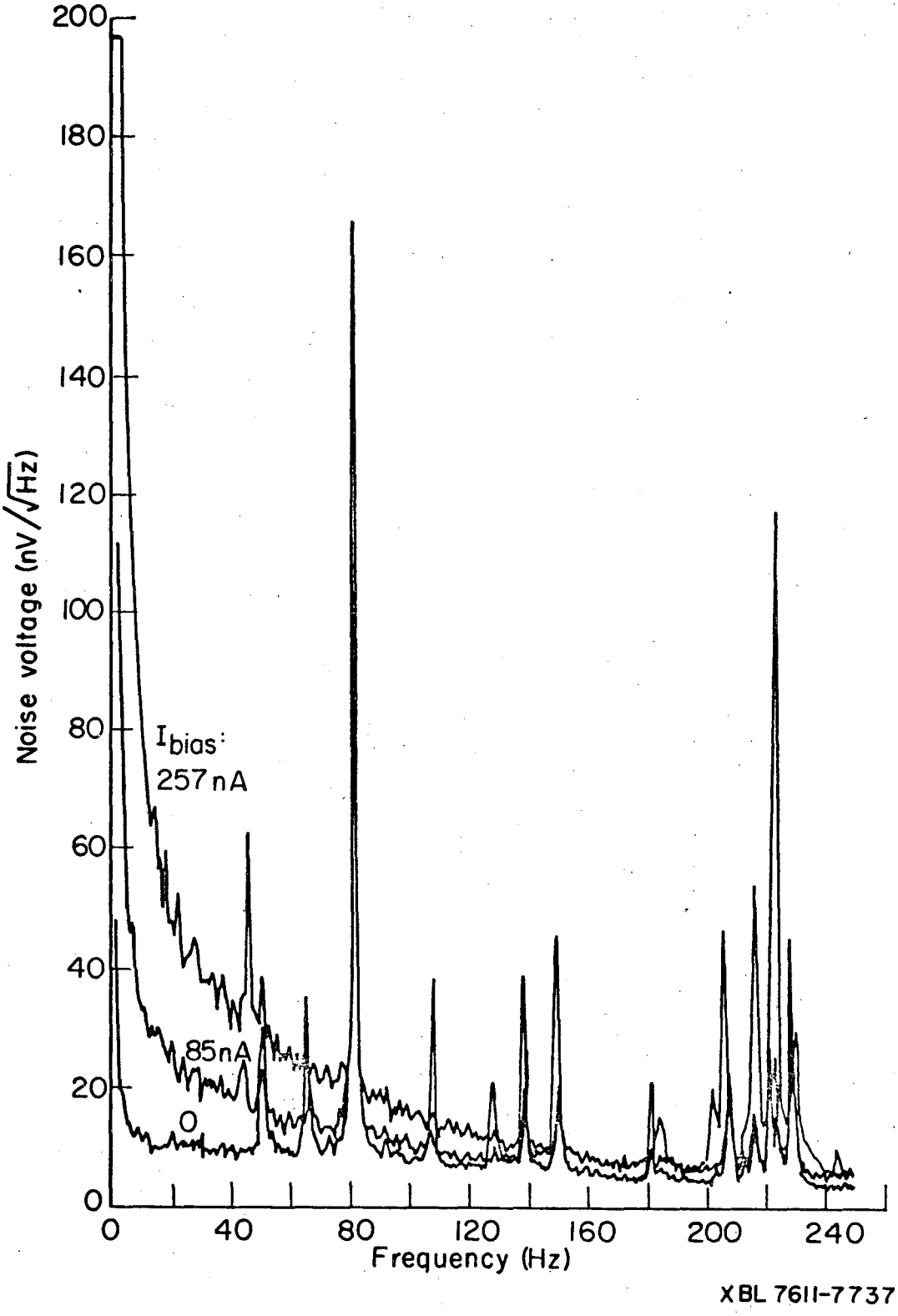

Fig. 5. Typical bolometer noise spectra. Notice the effect of increasing bias current. The peak at 80 Hz is due to a mechanical resonance.

E. Possible Improvements

It is of interest to determine what factors are limiting the performance of the bolometers we have built. With this information it may be possible to suggest future improvements. The bolometers are usually excess noise limited below $\sim$ 10 Hz. This noise is current dependent and has a 1/f power spectrum. If this excess noise is generated in the contacts then an alternate soldering procedure might eliminate it. On the other hand, if the noise is generated in the germanium itself then a different material must be procured or the preparation (cutting, etching, etc.) must be altered. The effect of various etching procedures was tested by varying both the length of time the germanium was etched and the composition of the etch. No strong correlation was evident from the tests. The noise appeared to be almost independent of the etching procedure used. Basically, if the surface of the germanium appeared smooth and shiny to the naked eye the etching was sufficient. However, it did appear that quenching the etch in methanol produced better results than quenching with distilled water.

In order to distinguish between noise generated in the contacts and noise that is generated in the germanium itself, a four terminal measurement was performed. Since the noise is current dependent a model of the noise as a fluctuating resistance seems reasonable (see Fig. 6). If the contact noise is the dominant noise mechanism then the noise observed across each pair of terminals would be quite different, since the current only flows through one pair of contacts (Fig. 6a). Alternatively, if the noise is intrinsic to the germanium then the voltages measured across

0 0 0 0 0 4 7 0 4 8 5 7 4 3

each pair will be comparable (Fig. 6b). The experiment showed that $V_1 \approx V_2$ in all cases, which suggests that the contacts are not the dominant noise source. When this result is combined with the fact that the noise is roughly etch independent, it suggests that the noise is internally generated in the germanium. Therefore, a new source of germanium may remove or reduce this noise source.

Another method of improving performance would be to lower the heat capacity. Using a smaller piece of germanium and a thinner sapphire substrate would help considerably. Alternately, diamond which has a lower specific heat (see Appendix B) could be used. If 0.001" thick sapphire were to be used instead of the present 0.005", the NEP could be lowered by about a factor of 3. Yet another improvement is the use of a lower temperature heat sink. Charcoal pumped ^{4}He or ^{3}He would lower the NEP by factors of 2 to 20. Finally, the development of a preamplifier with very low current noise ($\sim 10^{-16}$ amps/$\sqrt{\text{Hz}}$) would permit operation of higher resistance (or Δ) bolometers. These bolometers would have a higher responsivity.

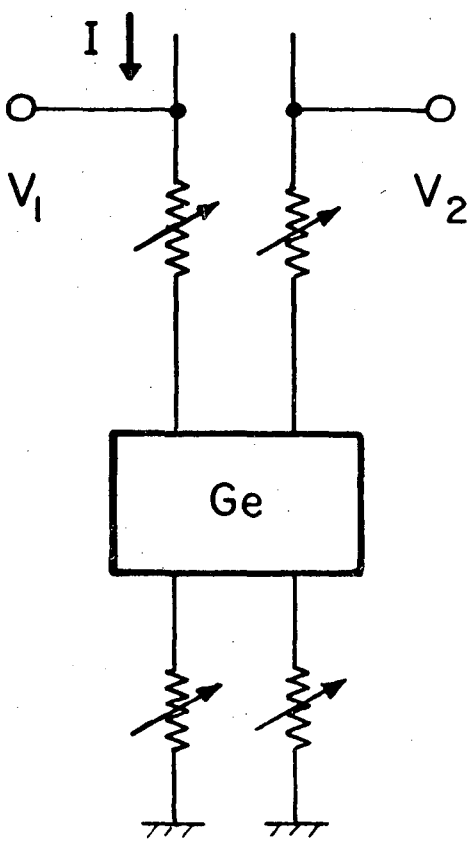

Contact noise dominant

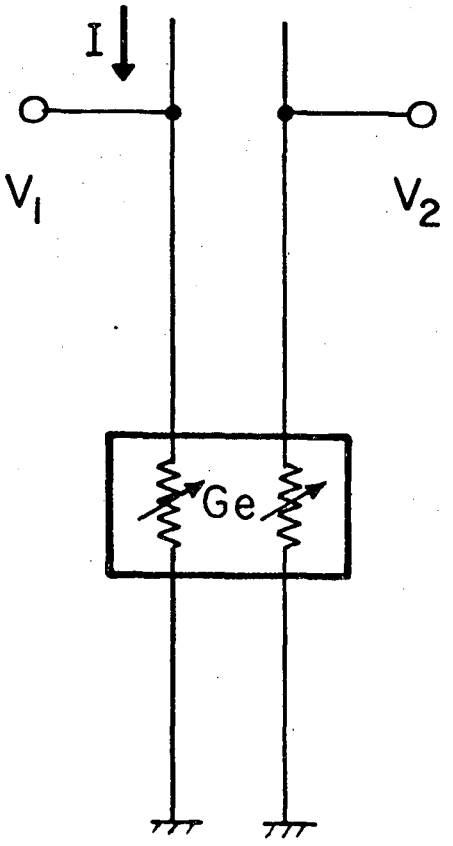

Intrinsic noise dominant

XBL 7611-7741

Fig. 6a. If the contact noise is dominant, then $V_1 >> V_2$.

Fig. 6b. If the intrinsic noise is dominant, $V_1 \sim V_2$.

Figure 6

0 0 0 0 9 7 0 3 5 3 4

IV. CONCLUSION

We have built composite semiconductor bolometers whose dark performance is typically $(NEP)_{dark} \sim 3 \times 10^{-14}$ W/$\sqrt{Hz}$ with an area of 4×4 mm. The absorptivity is ∿ 40%. This results in a detectivity ($\sqrt{area}$/NEP) of $D^* \sim 10^{13}$ cm $\sqrt{Hz}$/W. A factor of ∿ 3 improvement is anticipated with the availability of thinner sapphire substrates.

Although the detectivity of the best SNS critical current bolometers and superconducting transition edge (STE) bolometers are a factor of ∿ 10 times higher than these semiconductor bolometers, there are nevertheless some applications in which there are advantages in using a semiconductor bolometer. First of all, the electronics associated with a semiconductor bolometer are straightforward consisting only of an FET preamplifier and a bias supply, while the SNS and STE bolometers both require quite sophisticated electronics. In addition, the semiconductor bolometer will operate over rather large temperature ranges (albeit with reduced sensitivity) and thus operate over large ranges of background power. STE bolometers on the other hand, must operate at the superconducting transition temperature. Another advantage of the semiconductor bolometer is that it is capable of operating in high magnetic fields. The SNS and STE bolometers are of no value in the presence of high magnetic fields. In absorption measurements the semiconductor bolometer can be of value since the material under test can often be made into the substrate itself. Evaporated structures such as the SNS and STE bolometers can of course also be placed upon the material under test. However, the substrate appears to play an important role in the noise properties of these bolom-

eters[18]. Finally, neither the SNS nor the STE bolometer has yet shown the longevity necessary for reliable operation, although, progress is being made in this area. Any reduction in the excess noise will make the semiconductor bolometer even more competitive.

It should be pointed out that at any temperature the phonon fluctuation noise term in the NEP presents a fundamental limit to the dark NEP. This limit is $\sim 3 \times 10^{-15}$ W/$\sqrt{\text{Hz}}$ for T = 1.3 K and G = 10^{-7} W/K. For a low background system where the ideal NEP can be quite small ($\sim 10^{-16}$ W/$\sqrt{\text{Hz}}$) much lower bath temperatures will be required to reach the ideal limit. Thus, the next generation of bolometers will have to use pumped ^{3}He as the refrigerant in order to approach the ideal limit in low background environments.

0 0 0 0 9 7 8 0 8 7 8 5

APPENDIX A

Techniques for Computing the Background Fluctuation Noise and dc Radiation Power in a Frequency Interval

Given any frequency interval, the fluctuations in the incident power form a fundamental limit to the NEP of a detector system. This noise is the result of fluctuations in the number of photons arriving at the detector. A straightforward application of Bose-Einstein statistics yields the following formula for the background fluctuation limited NEP[19,20]

$$(NEP)^2_{BF} = \frac{4A\Omega(kT)^5B}{c^2h^3}\int \frac{\varepsilon_A\varepsilon_s x^4e^x}{(e^x - 1)^2}\,dx, \qquad (A\text{-}1)$$

where $A\Omega$ is the throughput of the detector system, B is the post detection bandwidth, ε_A is the emissivity of the absorber (detector), ε_s is the emissivity of the source, T is the source temperature and $x = h\nu c/kT$. Here ν is the wavenumber which is usually given in units of $[cm^{-1}]$.

In the Rayleigh-Jeans limit, $x << 1$ and $x^4e^x/(e^x - 1)^2 \approx x^2$ so that (A-1) becomes

$$(NEP)_{BF} \approx \frac{4A\Omega(kT)^5B}{c^2h^3}\int \varepsilon_A\varepsilon_s x^2dx\ . \qquad (A\text{-}2)$$

The background power incident upon the system is

$$P = \frac{2A\Omega(kT)^4}{c^2h^3}\int \frac{\varepsilon_A\varepsilon_s x^3}{e^x - 1}\,dx\ , \qquad (A\text{-}3)$$

which in the Rayleigh-Jeans limit becomes

$$P = \frac{2A\Omega(kT)^4}{c^2h^3}\int \varepsilon_A\varepsilon_s x^2dx\ . \qquad (A\text{-}4)$$

Combining (A-2) and (A-4) yields a convenient formula,

$$(NEP)^2_{BF} \simeq 2kTPB \qquad (x << 1) \ . \tag{A-5}$$

From (A-5) it is evident that the ultimate sensitivity of a bolometer system in the Rayleigh-Jeans limit is proportional to the square root of the incident background power.

In many cases, the Rayleigh-Jeans approximation is not appropriate. In these cases, (A-1) must be used. Evaluation of (A-1) must be done numerically. However, if we assume that the optical system exhibits a square spectral bandpass[21] we can simplify (A-1) and easily use tables to evaluate $(NEP)_{BF}$.

We begin by rewriting (A-1) as

$$(NEP)^2_{BF} = \frac{4(kT)^5 A\Omega}{c^2h^3} \ \varepsilon_A \varepsilon_s \int_{x_L}^{x_H} \frac{x^4 e^x}{(e^x - 1)^2} \, dx \ , \tag{A-6}$$

where ε_A, ε_s are now constant in the interval $x_L < x < x_H$ and are zero outside this interval. We next define the function

$$H(y) = \int_y^{\infty} \frac{x^4 e^x}{(e^x - 1)^2} \, dx \ , \tag{A-7}$$

so that (A-6) becomes

$$(NEP)^2_{BF} = \frac{4(kT)^5 A\Omega \varepsilon_A \varepsilon_s}{h^3 c^2} [H(x_L) - H(x_H)] \ , \tag{A-8}$$

$$\approx 7.684 \times 10^{-36} (T^5 A\Omega \varepsilon_A \varepsilon_s)[H(x_L) - H(x_H)] \ , \tag{A-9}$$

where $A\Omega$ is in [cm^2-sr]. The function H(x) is tabulated[22] in Table A-1.

It is also frequently of interest to be able to quickly and easily compute the background radiation power (A-3). This can be done in analogous

0 0 0 0 0 0 0 0 0 0 0 0

fashion as follows. We define

$$G(y) = \int_y^\infty \frac{x^3}{e^x - 1}\, dx \ . \tag{A-10}$$

If we again assume a square spectral bandpass between x_L and x_H, then (A-3) becomes

$$P = \frac{2A\Omega(kT)^4 \varepsilon_A \varepsilon_s}{c^2 h^3} [G(x_L) - G(x_H)] \ , \tag{A-11}$$

$$\approx 2.782 \times 10^{-13} \ (T^4 A\Omega \varepsilon_A \varepsilon_s)[G(x_L) - G(x_H)] \ , \tag{A-12}$$

where $A\Omega$ is in units of [cm^2-sr]. The function G(x) is also tabulated in Table A-1.

Table A-1

X	H(X)	H(0)-H(X)	G(X)	G(0)-G(X)
0.00	25.97575760	.00000001	6.49393940	.00000000
.05	25.97571595	.00004166	6.49389851	.00004089
.10	25.97542444	.00033316	6.49361840	.00032100
.15	25.97463387	.00112373	6.49287642	.00106298
.20	25.97309627	.00266134	6.49146740	.00247200
.25	25.97056552	.00519209	6.48920309	.00473632
.30	25.96679798	.00895963	6.48591145	.00802796
.35	25.96155310	.01420451	6.48143611	.01250329
.40	25.95459397	.02116363	6.47563573	.01830368
.45	25.94568795	.03006966	6.46838338	.02555602
.50	25.93460716	.04115045	6.45956595	.03437346
.55	25.92112910	.05462850	6.44908355	.04485585
.60	25.90503713	.07072048	6.43684892	.05709048
.65	25.88612096	.08963665	6.42278685	.07115255
.70	25.86417715	.11158045	6.40683360	.08710581
.75	25.83900959	.13674802	6.38893632	.10500308
.80	25.81042987	.16532774	6.36905253	.12488688
.85	25.77825771	.19749989	6.34714953	.14678987
.90	25.74232136	.23343624	6.32320390	.17072550
.95	25.70245790	.27329971	6.29720095	.19673845
1.00	25.65851356	.31724404	6.26913421	.22480519
1.05	25.61034404	.36541357	6.23900494	.25493447
1.10	25.55781469	.41794291	6.20682160	.28711780
1.15	25.50080082	.47495679	6.17259943	.32133998
1.20	25.43918780	.53656981	6.13635993	.35757947
1.25	25.37287126	.60288634	6.09813046	.39580894
1.30	25.30175722	.67400039	6.05794375	.43599565
1.35	25.22576215	.74999546	6.01583749	.47810191
1.40	25.14481302	.83094458	5.97185395	.52208546
1.45	25.05884739	.91691022	5.92603953	.56789987
1.50	24.96781332	1.00794429	5.87844442	.61549498
1.55	24.87166940	1.10408820	5.82912221	.66481719
1.60	24.77038466	1.20537294	5.77812954	.71580986
1.65	24.66393849	1.31181912	5.72552576	.76841365
1.70	24.55232048	1.42343713	5.67137258	.82256683
1.75	24.43553024	1.54022726	5.61573379	.87820561
1.80	24.31357768	1.66217992	5.55867497	.93526443
1.85	24.18648183	1.78927577	5.50026315	.99367625
1.90	24.05427162	1.92148598	5.44056659	1.05337281
1.95	23.91698515	2.05877246	5.37965450	1.11428490
2.00	23.77466951	2.20108810	5.31759681	1.17634260
2.05	23.62738052	2.34837709	5.25446391	1.23947549
2.10	23.47518244	2.50057517	5.19032649	1.30361291
2.15	23.31814765	2.65760996	5.12525527	1.36868414
2.20	23.15635632	2.81940129	5.05932084	1.43461856
2.25	22.98989409	2.98586151	4.99259349	1.50134591
2.30	22.81886172	3.15689588	4.92514303	1.56879638
2.35	22.64335472	3.33240289	4.85703862	1.63690079
2.40	22.46348299	3.51227461	4.78834865	1.70559076
2.45	22.27936048	3.69639713	4.71914059	1.77479881

Table A-1 (cont.)

X	H(X)	H(0)-H(X)	G(X)	G(0)-G(X)
2.50	22.09110675	3.88465086	4.64948089	1.84445851
2.55	21.89884665	4.07691095	4.57943482	1.91450458
2.60	21.70270992	4.27304768	4.50906643	1.98487297
2.65	21.50283080	4.47292681	4.43843840	2.05550100
2.70	21.29934763	4.67640997	4.36761199	2.12632741
2.75	21.09240252	4.88335509	4.29664696	2.19729244
2.80	20.88214091	5.09361670	4.22560150	2.26833790
2.85	20.66871123	5.30704637	4.15453215	2.33940725
2.90	20.45226455	5.52349306	4.08349380	2.41044560
2.95	20.23295415	5.74280346	4.01253960	2.48139980
3.00	20.01093521	5.96482239	3.94172095	2.55221845
3.05	19.78636446	6.18939314	3.87108746	2.62285195
3.10	19.55939982	6.41635779	3.80068692	2.69325248
3.15	19.33020005	6.64555755	3.73056531	2.76337409
3.20	19.09892447	6.87683313	3.66076676	2.83317265
3.25	18.86573260	7.11002500	3.59133355	2.90260585
3.30	18.63078390	7.34497371	3.52230613	2.97163327
3.35	18.39423741	7.58152020	3.45372310	3.04021630
3.40	18.15625155	7.81950606	3.38562121	3.10831819
3.45	17.91698379	8.05877382	3.31803542	3.17590398
3.50	17.67659042	8.29916719	3.25099886	3.24294055
3.55	17.43522628	8.54053133	3.18454286	3.30939654
3.60	17.19304455	8.78271305	3.11869702	3.37524238
3.65	16.95019654	9.02556107	3.05348918	3.44045023
3.70	16.70683142	9.26892619	2.98894545	3.50499395
3.75	16.46309610	9.51266151	2.92509030	3.56884910
3.80	16.21913500	9.75662261	2.86194652	3.63199289
3.85	15.97508988	10.00066772	2.79953528	3.69440412
3.90	15.73109972	10.24465788	2.73787620	3.75606320
3.95	15.48730053	10.48845709	2.67698733	3.81695207
4.00	15.24382522	10.73193239	2.61688524	3.87705416
4.05	15.00090351	10.97495410	2.55758502	3.93635438
4.10	14.75836179	11.21739582	2.49910035	3.99483906
4.15	14.51662304	11.45913456	2.44144352	4.05249588
4.20	14.27570673	11.70005088	2.38462549	4.10931391
4.25	14.03572873	11.94002887	2.32865594	4.16528346
4.30	13.79680128	12.17895632	2.27354327	4.22039613
4.35	13.55903291	12.41672470	2.21929470	4.27464470
4.40	13.32252837	12.65322923	2.16591627	4.32802314
4.45	13.08738866	12.88836895	2.11341290	4.38052650
4.50	12.85371093	13.12204668	2.06178845	4.43215095
4.55	12.62158850	13.35416910	2.01104574	4.48289367
4.60	12.39111086	13.58464675	1.96118658	4.53275282
4.65	12.16236361	13.81339399	1.91221186	4.58172754
4.70	11.93542855	14.04032905	1.86412156	4.62981784
4.75	11.71038361	14.26537399	1.81691478	4.67702462
4.80	11.48730293	14.48845468	1.77058982	4.72334959
4.85	11.26625683	14.70950078	1.72514416	4.76879524
4.90	11.04731189	14.92844571	1.68057459	4.81336481
4.95	10.83053099	15.14522662	1.63687715	4.85706225

Table A-1 (cont.)

X	H(X)	H(0)-H(X)	G(X)	G(0)-G(X)
5.00	10.61597329	15.35978431	1.59404724	4.89989216
5.05	10.40369425	15.57206326	1.55207962	4.94185978
5.10	10.19374614	15.78201147	1.51096846	4.98297095
5.15	9.98617710	15.98958051	1.47070736	5.02323204
5.20	9.78103221	16.19472539	1.43128941	5.06264999
5.25	9.57835308	16.39740452	1.39270722	5.10123218
5.30	9.37817795	16.59757966	1.35495293	5.13899648
5.35	9.18054182	16.79521579	1.31801824	5.17592116
5.40	8.98547649	16.99028112	1.28189448	5.21204492
5.45	8.79301066	17.18274695	1.24657260	5.24736680
5.50	8.60316998	17.37258763	1.21204322	5.28189618
5.55	8.41597715	17.55978046	1.17829664	5.31564276
5.60	8.23145199	17.74430561	1.14532290	5.34861650
5.65	8.04961154	17.92614607	1.11311176	5.38082764
5.70	7.87047009	18.10528751	1.08165275	5.41228665
5.75	7.69403935	18.28171826	1.05093520	5.44300420
5.80	7.52032844	18.45542917	1.02094826	5.47299115
5.85	7.34934404	18.62641356	.99168089	5.50225851
5.90	7.18109046	18.79466714	.96312194	5.53081746
5.95	7.01556971	18.96018789	.93526011	5.55867929
6.00	6.85278159	19.12297601	.90808402	5.58585538
6.05	6.69272379	19.28303382	.88158218	5.61235722
6.10	6.53539195	19.44036566	.85574305	5.63819635
6.15	6.38077975	19.59497785	.83055504	5.66338436
6.20	6.22887902	19.74687859	.80600650	5.68793291
6.25	6.07967978	19.89607783	.78208578	5.71185362
6.30	5.93317034	20.04258727	.75878122	5.73515818
6.35	5.78933738	20.18642022	.73608117	5.75785823
6.40	5.64816604	20.32759157	.71397400	5.77996540
6.45	5.50963997	20.46611764	.69244809	5.80149131
6.50	5.37374143	20.60201619	.67149190	5.82244750
6.55	5.24045131	20.73530629	.65109390	5.84284550
6.60	5.10974934	20.86600827	.63124266	5.86269674
6.65	4.98161398	20.99414362	.61192681	5.88201259
6.70	4.85602263	21.11973498	.59313505	5.90080435
6.75	4.73295162	21.24280599	.57485619	5.91908321
6.80	4.61237630	21.36338130	.55707912	5.93686028
6.85	4.49427114	21.48148646	.53979284	5.95414656
6.90	4.37860973	21.59714787	.52298646	5.97095294
6.95	4.26536489	21.71039272	.50664921	5.98729019
7.00	4.15450969	21.82124892	.49077044	6.00316896
7.05	4.04601254	21.92974506	.47533963	6.01359978
7.10	3.93984726	22.03591035	.46034637	6.03359303
7.15	3.83598307	22.13977453	.44578043	6.04815897
7.20	3.73438971	22.24136790	.43163168	6.06230772
7.25	3.63502644	22.34072116	.41789014	6.07604926
7.30	3.53789214	22.43786547	.40454600	6.08939340
7.35	3.44292530	22.53283230	.39158957	6.10234983
7.40	3.35010412	22.62565348	.37901133	6.11492807
7.45	3.25939651	22.71636110	.36680189	6.12713751

X	H(X)	H(0)-H(X)	G(X)	G(0)-G(X)
7.50	3.17077016	22.80498745	.35495205	6.13898735
7.55	3.08419256	22.89156505	.34345274	6.15048666
7.60	2.99963106	22.97612655	.33229505	6.16164435
7.65	2.91705289	23.05870471	.32147023	6.17246917
7.70	2.83642522	23.13933239	.31096970	6.18296970
7.75	2.75771514	23.21804247	.30078503	6.19315437
7.80	2.68088976	23.29486785	.29090794	6.20303146
7.85	2.60591619	23.36984141	.28133033	6.21260907
7.90	2.53276161	23.44299600	.27204424	6.22189517
7.95	2.46139325	23.51436436	.26304187	6.23089753
8.00	2.39177845	23.58397915	.25431561	6.23962379
8.05	2.32388470	23.65187291	.24585796	6.24808144
8.10	2.25767961	23.71807799	.23766160	6.25627780
8.15	2.19313099	23.78262661	.22971938	6.26422002
8.20	2.13020683	23.84555078	.22202428	6.27191512
8.25	2.06887534	23.90688227	.21456944	6.27936996
8.30	2.00910496	23.96665265	.20734816	6.28659124
8.35	1.95086439	24.02489322	.20035388	6.29358552
8.40	1.89412260	24.08163501	.19358020	6.30035921
8.45	1.83884882	24.13690878	.18702085	6.30691856
8.50	1.78501261	24.19074499	.18066972	6.31326969
8.55	1.73258383	24.24317377	.17452083	6.31941857
8.60	1.68153265	24.29422495	.16856837	6.32537103
8.65	1.63182960	24.34392801	.16280665	6.33113276
8.70	1.58344552	24.39231208	.15723010	6.33670931
8.75	1.53635165	24.43940596	.15183331	6.34210609
8.80	1.49051955	24.48523806	.14661100	6.34732840
8.85	1.44592118	24.52983643	.14155803	6.35238137
8.90	1.40252887	24.57322874	.13666936	6.35727004
8.95	1.36031533	24.61544228	.13194011	6.36199929
9.00	1.31925367	24.65650393	.12736550	6.36657390
9.05	1.27931740	24.69644020	.12294090	6.37099851
9.10	1.24048041	24.73527719	.11866176	6.37527764
9.15	1.20271702	24.77304059	.11452370	6.37941571
9.20	1.16600192	24.80975569	.11053240	6.38341700
9.25	1.13031025	24.84544736	.10665371	6.38728569
9.30	1.09561753	24.88014009	.10291355	6.39102585
9.35	1.06189971	24.91385790	.09929796	6.39464144
9.40	1.02913315	24.94662446	.09580311	6.39813629
9.45	.99729462	24.97846299	.09242524	6.40151416
9.50	.96636131	25.00939630	.08916071	6.40477869
9.55	.93631081	25.03944680	.08600598	6.40793342
9.60	.90712114	25.06863646	.08295762	6.41098178
9.65	.87877072	25.09698688	.08001227	6.41392713
9.70	.85123830	25.12451921	.07716669	6.41677271
9.75	.82450339	25.15125422	.07441771	6.41952169
9.80	.79854535	25.17721226	.07176227	6.42217713
9.85	.77334434	25.20241327	.06919739	6.42474202
9.90	.74888080	25.22687680	.06672016	6.42721925
9.95	.72513559	25.25062202	.06432777	6.42961163

Table A-1 (cont.)

X	H(X)	H(0)-H(X)	G(X)	G(0)-G(X)
10.00	.70208993	25.27366767	.06201751	6.43192190
10.05	.67972548	25.29603213	.05978670	6.43415270
10.10	.65802423	25.31773337	.05763279	6.43630661
10.15	.63696361	25.33878900	.05555328	6.43838612
10.20	.61654139	25.35921622	.05354574	6.44039366
10.25	.59672572	25.37903189	.05160782	6.44233158
10.30	.57750513	25.39825247	.04973724	6.44420216
10.35	.55886352	25.41689409	.04793179	6.44600761
10.40	.54078513	25.43497248	.04618932	6.44775008
10.45	.52325459	25.45250303	.04450776	6.44943164
10.50	.50625682	25.46950078	.04288509	6.45105432
10.55	.48977717	25.48598044	.04131934	6.45262006
10.60	.47380127	25.50195634	.03980864	6.45413077
10.65	.45831510	25.51744251	.03835113	6.45558827
10.70	.44330498	25.53245263	.03694504	6.45699436
10.75	.42875755	25.54700006	.03559865	6.45835075
10.80	.41465977	25.56109783	.03428029	6.45966912
10.85	.40099893	25.57475868	.03301832	6.46092109
10.90	.38776260	25.58799501	.03180119	6.46213821
10.95	.37493868	25.60081893	.03062738	6.46331202
11.00	.36251535	25.61324225	.02949542	6.46444398
11.05	.35048111	25.62527650	.02840388	6.46553552
11.10	.33882472	25.63693288	.02735138	6.46658802
11.15	.32753524	25.64822236	.02633660	6.46760280
11.20	.31660201	25.65915560	.02535824	6.46858117
11.25	.30601462	25.66974298	.02441504	6.46952436
11.30	.29576296	25.67999465	.02350580	6.47043360
11.35	.28583715	25.68992045	.02262935	6.47131005
11.40	.27622759	25.69953001	.02178455	6.47215485
11.45	.26692492	25.70883268	.02097031	6.47296909
11.50	.25792003	25.71783757	.02018557	6.47375383
11.55	.24920405	25.72655356	.01942930	6.47451010
11.60	.24076834	25.73498926	.01870051	6.47523889
11.65	.23260450	25.74315310	.01799824	6.47594116
11.70	.22470436	25.75105325	.01732156	6.47661784
11.75	.21705995	25.75869766	.01666958	6.47726982
11.80	.20966353	25.76609407	.01604144	6.47789797
11.85	.20250758	25.77325002	.01543628	6.47850312
11.90	.19558478	25.78017283	.01485330	6.47908610
11.95	.18888799	25.78686961	.01429172	6.47964768
12.00	.18241031	25.79334730	.01375078	6.48018862
12.05	.17614499	25.79961262	.01322976	6.48070965
12.10	.17008549	25.80567212	.01272793	6.48121147
12.15	.16422545	25.81153215	.01224463	6.48169479
12.20	.15855870	25.81719890	.01177918	6.48216022
12.25	.15307923	25.82267838	.01133096	6.48260844
12.30	.14778119	25.82797641	.01089934	6.48304006
12.35	.14265893	25.83309867	.01048374	6.48345566
12.40	.13770694	25.83805066	.01008358	6.48385583
12.45	.13291987	25.84283773	.00969829	6.48424111

Table A-1 (cont.)

X	H(X)	H(0)-H(X)	G(X)	G(0)-G(X)
12.50	.12829253	25.84746507	.00932736	6.48461204
12.55	.12381988	25.85193773	.00897026	6.48496914
12.60	.11949701	25.85626060	.00862649	6.48531291
12.65	.11531918	25.86043842	.00829557	6.48564383
12.70	.11128178	25.86447583	.00797704	6.48596237
12.75	.10738032	25.86837728	.00767043	6.48626897
12.80	.10361047	25.87214713	.00737534	6.48656407
12.85	.09996801	25.87578960	.00709132	6.48684808
12.90	.09644884	25.87930877	.00681798	6.48712142
12.95	.09304900	25.88270861	.00655494	6.48738446
13.00	.08976463	25.88599297	.00630180	6.48763760
13.05	.08659201	25.88916559	.00605822	6.48788118
13.10	.08352752	25.89223009	.00582384	6.48811556
13.15	.08056763	25.89518997	.00559833	6.48834108
13.20	.07770896	25.89804865	.00538135	6.48855806
13.25	.07494818	25.90080942	.00517259	6.48876681
13.30	.07228211	25.90347549	.00497175	6.48896765
13.35	.06970765	25.90604996	.00477855	6.48916086
13.40	.06722177	25.90853583	.00459268	6.48934672
13.45	.06482158	25.91093603	.00441390	6.48952551
13.50	.06250424	25.91325337	.00424192	6.48969748
13.55	.06026702	25.91549059	.00407651	6.48986290
13.60	.05810726	25.91765034	.00391741	6.49002200
13.65	.05602241	25.91973520	.00376439	6.49017501
13.70	.05400996	25.92174765	.00361722	6.49032218
13.75	.05206751	25.92369010	.00347570	6.49046371
13.80	.05019271	25.92556499	.00333959	6.49059981
13.85	.04838333	25.92737428	.00320871	6.49073069
13.90	.04663715	25.92912046	.00308286	6.49085654
13.95	.04495206	25.93080555	.00296185	6.49097755
14.00	.04332600	25.93243160	.00284549	6.49109391
14.05	.04175700	25.93400061	.00273362	6.49120578
14.10	.04024312	25.93551449	.00262606	6.49131334
14.15	.03878250	25.93697511	.00252265	6.49141675
14.20	.03737334	25.93838427	.00242324	6.49151616
14.25	.03601389	25.93974372	.00232767	6.49161173
14.30	.03470246	25.94105515	.00223580	6.49170360
14.35	.03343742	25.94232018	.00214749	6.49179191
14.40	.03221719	25.94354041	.00206260	6.49187680
14.45	.03104024	25.94471736	.00198101	6.49195839
14.50	.02990509	25.94585252	.00190259	6.49203681
14.55	.02881030	25.94694731	.00182722	6.49211219
14.60	.02775449	25.94800312	.00175477	6.49218463
14.65	.02673632	25.94902129	.00168516	6.49225425
14.70	.02575449	25.95000311	.00161825	6.49232115
14.75	.02480776	25.95094985	.00155396	6.49238545
14.80	.02389490	25.95186270	.00149217	6.49244723
14.85	.02301475	25.95274285	.00143280	6.49250660
14.90	.02216617	25.95359143	.00137575	6.49256365
14.95	.02134808	25.95440953	.00132094	6.49261846

Table A-1 (cont.)

X	H(X)	H(0)-H(X)	G(X)	G(0)-G(X)
15.00	.02055939	25.95519821	.00126827	6.49267113
15.05	.01979911	25.95595850	.00121767	6.49272173
15.10	.01906623	25.95669138	.00116905	6.49277035
15.15	.01835979	25.95739781	.00112235	6.49281706
15.20	.01767888	25.95807872	.00107748	6.49286193
15.25	.01702260	25.95873500	.00103437	6.49290503
15.30	.01639009	25.95936752	.00099296	6.49294644
15.35	.01578050	25.95997710	.00095318	6.49298622
15.40	.01519304	25.96056456	.00091497	6.49302443
15.45	.01462693	25.96113067	.00087827	6.49306113
15.50	.01408141	25.96167619	.00084302	6.49309638
15.55	.01355575	25.96220185	.00080916	6.49313024
15.60	.01304927	25.96270833	.00077664	6.49316276
15.65	.01256127	25.96319634	.00074541	6.49319399
15.70	.01209109	25.96366651	.00071541	6.49322399
15.75	.01163812	25.96411949	.00068661	6.49325279
15.80	.01120172	25.96455588	.00065894	6.49328046
15.85	.01078133	25.96497628	.00063238	6.49330702
15.90	.01037636	25.96538125	.00060687	6.49333253
15.95	.00998626	25.96577135	.00058237	6.49335703
16.00	.00961050	25.96614710	.00055885	6.49338055
16.05	.00924858	25.96650903	.00053626	6.49340314
16.10	.00889999	25.96685762	.00051458	6.49342482
16.15	.00856426	25.96719335	.00049376	6.49344564
16.20	.00824092	25.96751669	.00047377	6.49346562
16.25	.00792953	25.96782808	.00045458	6.49348483
16.30	.00762965	25.96812795	.00043615	6.49350325
16.35	.00734088	25.96841672	.00041846	6.49352094
16.40	.00706282	25.96869479	.00040148	6.49353792
16.45	.00679507	25.96896254	.00038518	6.49355422
16.50	.00653726	25.96922035	.00036953	6.49356987
16.55	.00628904	25.96946857	.00035451	6.49358489
16.60	.00605005	25.96970756	.00034009	6.49359931
16.65	.00581996	25.96993765	.00032625	6.49361315
16.70	.00559844	25.97015916	.00031297	6.49362644
16.75	.00538520	25.97037241	.00030021	6.49363919
16.80	.00517991	25.97057769	.00028798	6.49365142
16.85	.00498230	25.97077530	.00027623	6.49366317
16.90	.00479208	25.97096552	.00026496	6.49367444
16.95	.00460899	25.97114862	.00025414	6.49368526
17.00	.00443276	25.97132485	.00024376	6.49369564
17.05	.00426313	25.97149447	.00023380	6.49370561
17.10	.00409988	25.97165772	.00022424	6.49371517
17.15	.00394276	25.97181484	.00021506	6.49372434
17.20	.00379156	25.97196605	.00020626	6.49373315
17.25	.00364604	25.97211157	.00019781	6.49374159
17.30	.00350601	25.97225160	.00018970	6.49374970
17.35	.00337125	25.97238635	.00018192	6.49375748
17.40	.00324159	25.97251602	.00017446	6.49376494
17.45	.00311682	25.97264079	.00016730	6.49377210

Table A-1 (cont.)

X	H(X)	H(0)-H(X)	G(X)	G(0)-G(X)
17.50	.00299677	25.97276084	.00016043	6.49377807
17.55	.00288126	25.97287635	.00015394	6.49378556
17.60	.00277012	25.97298748	.00014752	6.49379189
17.65	.00266320	25.97309441	.00014145	6.49379795
17.70	.00256033	25.97319728	.00013563	6.49380377
17.75	.00246137	25.97329624	.00013005	6.49380936
17.80	.00236616	25.97339144	.00012469	6.49381471
17.85	.00227458	25.97348302	.00011955	6.49381985
17.90	.00218648	25.97357112	.00011462	6.49382478
17.95	.00210174	25.97365587	.00010990	6.49382951
18.00	.00202023	25.97373738	.00010536	6.49383404
18.05	.00194182	25.97381578	.00010101	6.49383839
18.10	.00186641	25.97389120	.00009684	6.49384256
18.15	.00179388	25.97396373	.00009284	6.49384656
18.20	.00172412	25.97403348	.00008900	6.49385040
18.25	.00165703	25.97410057	.00008532	6.49385408
18.30	.00159251	25.97416509	.00008179	6.49385761
18.35	.00153047	25.97422714	.00007840	6.49386100
18.40	.00147080	25.97428681	.00007515	6.49386425
18.45	.00141342	25.97434419	.00007204	6.49386736
18.50	.00135824	25.97439936	.00006905	6.49387035
18.55	.00130519	25.97445242	.00006619	6.49387321
18.60	.00125417	25.97450343	.00006344	6.49387596
18.65	.00120512	25.97455248	.00006081	6.49387859
18.70	.00115796	25.97459965	.00005828	6.49388112
18.75	.00111262	25.97464499	.00005586	6.49388354
18.80	.00106902	25.97468858	.00005354	6.49388586
18.85	.00102711	25.97473050	.00005131	6.49388809
18.90	.00098682	25.97477079	.00004918	6.49389022
18.95	.00094808	25.97480953	.00004713	6.49389227
19.00	.00091084	25.97484677	.00004517	6.49389423
19.05	.00087504	25.97488256	.00004329	6.49389611
19.10	.00084063	25.97491697	.00004148	6.49389792
19.15	.00080756	25.97495005	.00003975	6.49389965
19.20	.00077576	25.97498184	.00003810	6.49390130
19.25	.00074520	25.97501240	.00003651	6.49390289
19.30	.00071583	25.97504178	.00003498	6.49390442
19.35	.00068760	25.97507001	.00003352	6.49390588
19.40	.00066047	25.97509714	.00003212	6.49390728
19.45	.00063439	25.97512322	.00003078	6.49390862
19.50	.00060932	25.97514828	.00002949	6.49390991
19.55	.00058524	25.97517237	.00002826	6.49391114
19.60	.00056209	25.97519551	.00002708	6.49391233
19.65	.00053985	25.97521776	.00002594	6.49391346
19.70	.00051847	25.97523913	.00002486	6.49391455
19.75	.00049793	25.97525967	.00002381	6.49391559
19.80	.00047820	25.97527941	.00002282	6.49391658
19.85	.00045923	25.97529838	.00002186	6.49391754
19.90	.00044101	25.97531660	.00002094	6.49391846
19.95	.00042350	25.97533411	.00002006	6.49391934

APPENDIX B

Low Temperature Properties of Common Bolometer Construction Materials

Knowledge of the thermal conductivity and specific heat of bolometer construction materials is of importance in designing bolometers. The table presented in this appendix lists approximate values of these two quantities at three different temperatures for some typical bolometer construction materials. The table has been compiled from a variety of different sources and personal communications. It should be kept in mind that these values are approximate and may vary from sample to sample.

Material	T = 1.5 K		T = 3.5 K		T = 5 K		Density ρ
	g	c	g	c	g	c	
Sapphire	0.06	1×10^{-6}	0.4	2×10^{-5}	1	6×10^{-5}	4.0
Nylon	4×10^{-5}	6×10^{-5}	1×10^{-4}	1×10^{-4}	2×10^{-4}	1.4×10^{-4}	
Copper	2	2×10^{-4}	6	6×10^{-4}	8	1×10^{-3}	8.9
Aluminum	8	2×10^{-4}	15	5×10^{-4}	20	1×10^{-3}	2.7
Indium	4	4×10^{-4}	8	4×10^{-3}	8	1×10^{-2}	7.3
Tin	1	1×10^{-4}	4	2×10^{-3}	25	4×10^{-3}	7.3
Lead	0.4	5×10^{-4}	3	6×10^{-3}	12	1×10^{-2}	11.3
Bismuth		2×10^{-4}		3×10^{-3}	0.1	1×10^{-2}	9.8
Diamond	0.02	5×10^{-8}	0.3	6×10^{-7}	0.7	2×10^{-6}	3.5
Niobium	8×10^{3}	4×10^{-5}	3×10^{-2}	1×10^{-3}	5×10^{-2}	5×10^{-3}	8.6
Tantalum	1×10^{-2}	5×10^{-4}	4×10^{-2}	2×10^{-3}	6×10^{-2}	4×10^{-3}	16.6
Teflon				3×10^{-2}	6×10^{-4}		2.1
Pyrex		2×10^{-5}		3×10^{-4}		0.1	
Germanium		9×10^{-6}		1×10^{-4}		3×10^{-4}	5.3
Quartz (fused)					1×10^{-3}		
Quartz (crystal)		2×10^{-6}			7		2.2
Mylar							1.4
Brass					2×10^{-2}		
SS304					3×10^{-3}		
50-50 PbSn Solder			0.15		0.21		

g in $[\frac{W}{cm-K}]$ c in $[\frac{J}{K-cm^3}]$

APPENDIX C

Alternate Techniques for Measuring Bolometer Responsivity

An alternate expression for the electrical responsivity S of a bolometer can be derived in terms of the ac and dc impedances of the bolometer. Mather[23] derives a somewhat restricted version of this formula. Jones[17] appears to be the first to have derived the following expression:

$$S(\omega) = \frac{1}{2I} \frac{(\frac{Z(\omega)}{R} - 1)}{(\frac{Z(\omega)}{Z_L(\omega)} + 1)} . \qquad \text{(C-1)}$$

In this expression, I is the bias current, $Z(\omega) = dV/dI$ is the ac impedance of the bolometer, $R = V/I$ is the dc impedance of the bolometer and $Z_L(\omega)$ is the ac load impedance. For the case of a bolometer biased with a constant current, (C-1) reduces to

$$S(\omega) = \frac{1}{2I} (\frac{Z(\omega)}{R} - 1) \qquad (Z_L \to \infty) . \qquad \text{(C-2)}$$

Examination of (C-1) or (C-2) reveals that a measurement of the ac and dc bolometer impedances and the bias current is sufficient to determine the electrical responsivity. The ac impedance of the bolometer is easily measured with a lock-in amplifier. Figure C-1 illustrates the technique we employ. The dc component of V_I determines the dc bias current I. The dc component of V_B determines the dc resistance of the bolometer, $R = V_B(0)/I$. V_{ac} is selected to be much smaller than V_{dc} and R_L is assumed to be completely resistive. The ac impedance of the bolometer is $Z(\omega) =$

0 00 00 07 40 74 07 00 64 86 38 2

$V_B(\omega)\ R_L/V_I(\omega)$. Note that $V_B(\omega)$ and $V_I(\omega)$ are complex numbers having both an amplitude as well as a phase.

Alternatively a bridge circuit[17,23] can be used to measure the responsivity. Figure C-2 is a schematic diagram of the circuit that we use. We assume that R_1, R_2, and R_L are purely resistive. In use, the bridge is adjusted so that $V_{BD} = 0$ when $V_{sig} = 0$. This implies that

$$\frac{R_2}{R_1 + R_2} = \frac{R}{R + R_L} , \tag{C-3}$$

where we have neglected R_3 in comparison to R_L. Next, the ac voltage $V_{BD}(w)$ is measured with $V_{sig} \neq 0$. This voltage is

$$V_{BD} = \left(\frac{Z}{Z + R_L} - \frac{R}{R_1 + R_2}\right) V_{sig}$$

$$= \left(\frac{Z}{Z + R_L} - \frac{R}{R + R_L}\right) V_{sig} , \tag{C-4}$$

where we have used (C-3).

Substituting (C-1) into (C-4) yields

$$S(\omega) = \frac{R + R_L}{2IR} \frac{V_{BD}}{V_{AC}} . \tag{C-5}$$

Noting that $V_{BC} = V_{AC}\ R/(R + R_L)$, we can simplify (C-5) so that

$$S(\omega) = \frac{R_3 V_{BD}(\omega)}{V_I(0)\ V_{BC}(\omega)} \left[\frac{\text{volts}}{\text{watt}}\right] . \tag{C-6}$$

Unfortunately, we have not had good success in measuring the responsivity of bolometers whose responsivity is above $\sim 6 \times 10^5$ V/W with this method. This is due to problems in balancing the bridge precisely and also due to the stray capacitance and inductance of the cryogenic cabling and load resistor.

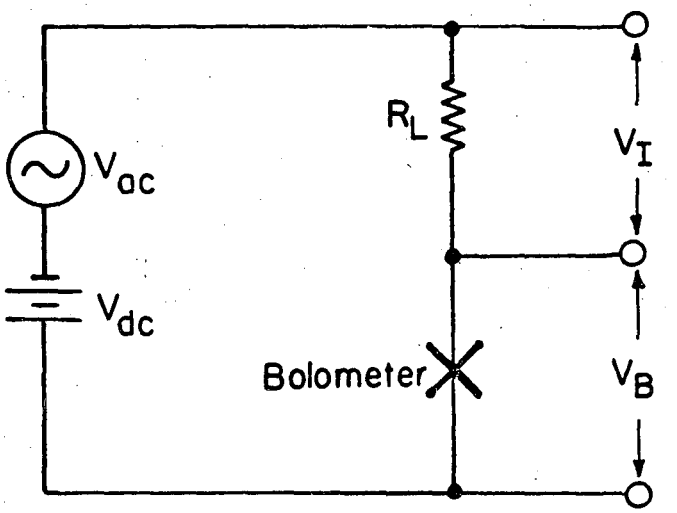

Fig. C-1. A technique for measuring $Z(\omega)$.

$$Z(\omega) = V_B(\omega)\ R_L/V_I(\omega).$$

0 00 00 00 40 74 07 00 64 85 48 3

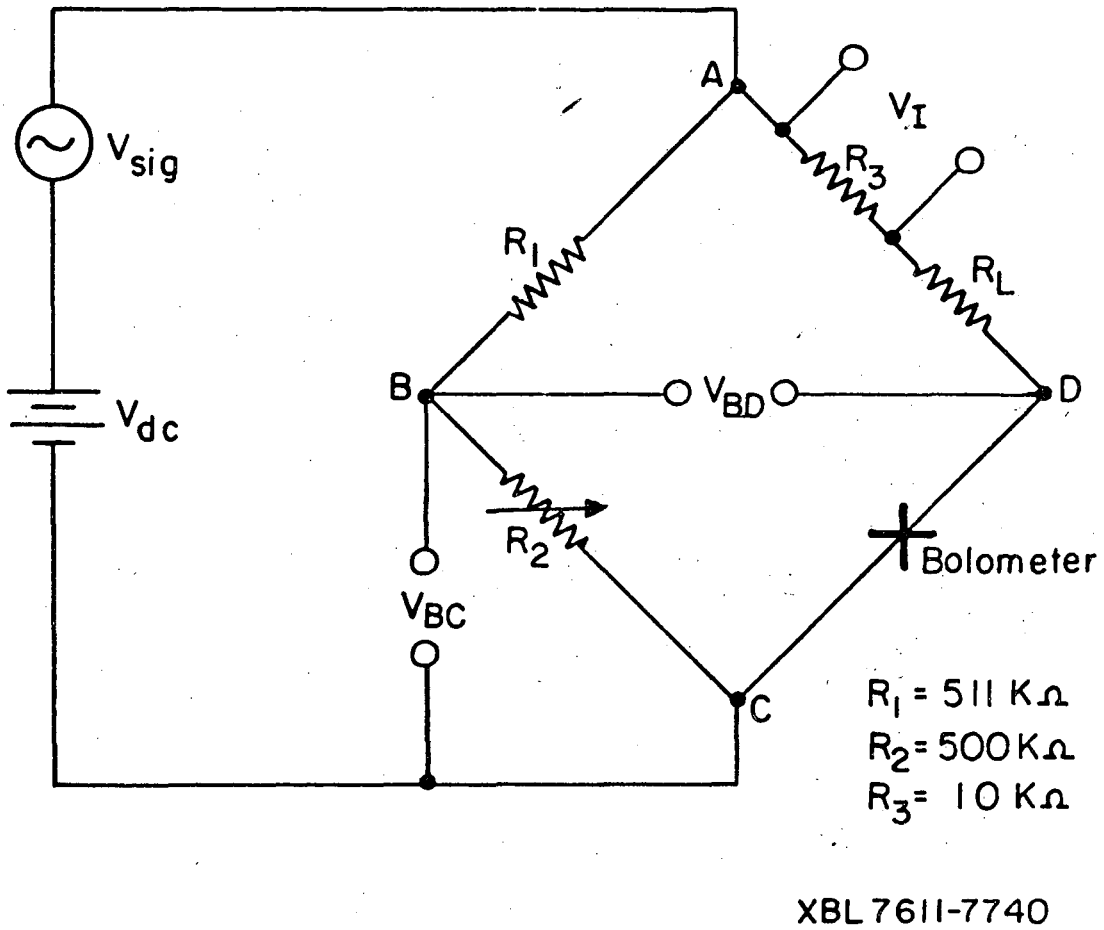

Fig. C-2. Jones' bolometer bridge circuit.

Footnotes and References

1. W. Herschel, Phil. Trans. R. Soc. 90, 284 (1800).

2. S. P. Langley, Infrared Phys. 3, 195 (1963).

3. F. J. Low, J. Opt. Soc. Am. 51, 1300 (1961).

4. J. Clarke, G. I. Hoffer, and P. L. Richards, Revue de Physique Appliquée 9, 69 (1974).

5. G. I. Hoffer, Ph.D. thesis, University of California, LBL-3759 (1975).

6. D. H. Andrews, R. M. Milton, and W. DeSorbo, J. Opt. Soc. Am. 36, 518 (1946).

7. J. Clarke, G. I. Hoffer, P. L. Richards, and N.-H. Yeh, Fourteenth International Conference on Low Temperature Physics (1975).

8. For example, the Molectron Corp. has coated its silicon bolometers with a layer of chromium in an attempt to increase absorption. The results of this technique are at present ambiguous. Silicon and copper have also been tried as substrate materials.

9. F. J. Low and A. P. Hoffman, Appl. Optics 2, 649 (1963).

10. C. Kittel, Introduction to Solid State Physics, 4th ed. (John Wiley and Sons, New York, 1971), p. 263.

11. R. L. Garwin, Rev. Sci. Instr. 27, 820 (1956).

12. D. P. Woody, Ph.D. thesis, University of California, LBL-4188 (1975).

13. M. J. D. Powell, The Computer Journal 7, 155 (1964).

14. J. A. Nelder and R. Mead, The Computer Journal 7, 308 (1965).

15. Actually γ is proportional to $1/T^2$ for semiconductor bolometers. However, for $T \approx T_s$ the assumption is quite adequate.

16. Note that $T^* << 1$ is necessary for (25) to be consistent with the assumption that $P_o >> I^2R$.

17. R. C. Jones, J. Opt. Soc. Am. 43, 1 (1953).

18. J. Clarke, personal communication.

19. W. B. Lewis, Proc. Phys. Soc. (London) 57, 34 (1947).

20. P. B. Fellgett, J. Opt. Soc. Am., 39, 970 (1949).

0 0 0 0 4 7 0 4 5 8 4

21. This assumption is not terribly severe since the frequency characteristic can always be approximated by a sequence of rectangles.

22. Series expansions of this function are given by W. L. Wolfe, Appl. Opt. 9, 2578 (1970).

23. J. C. Mather, Ph.D. thesis, University of California, LBL-2258 (1974).

This report was done with support from the United States Energy Research and Development Administration. Any conclusions or opinions expressed in this report represent solely those of the author(s) and not necessarily those of The Regents of the University of California, the Lawrence Berkeley Laboratory or the United States Energy Research and Development Administration.

TECHNICAL INFORMATION DIVISION
LAWRENCE BERKELEY LABORATORY
UNIVERSITY OF CALIFORNIA
BERKELEY, CALIFORNIA 94720